

低エネルギー反中性子散乱実験による 反中性子-陽子（原子核）間相互作用の研究

藤岡 宏之（東京科学大学）

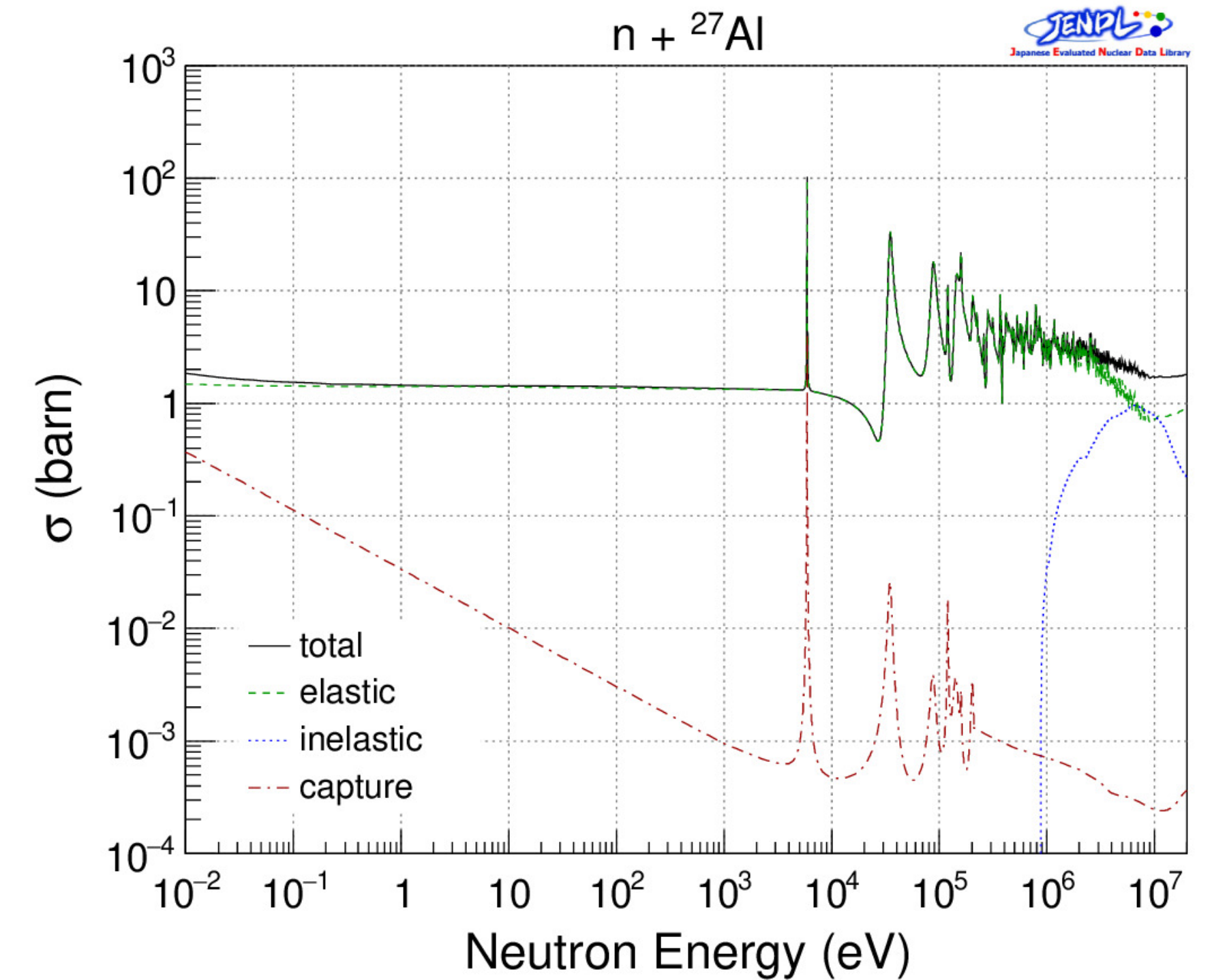
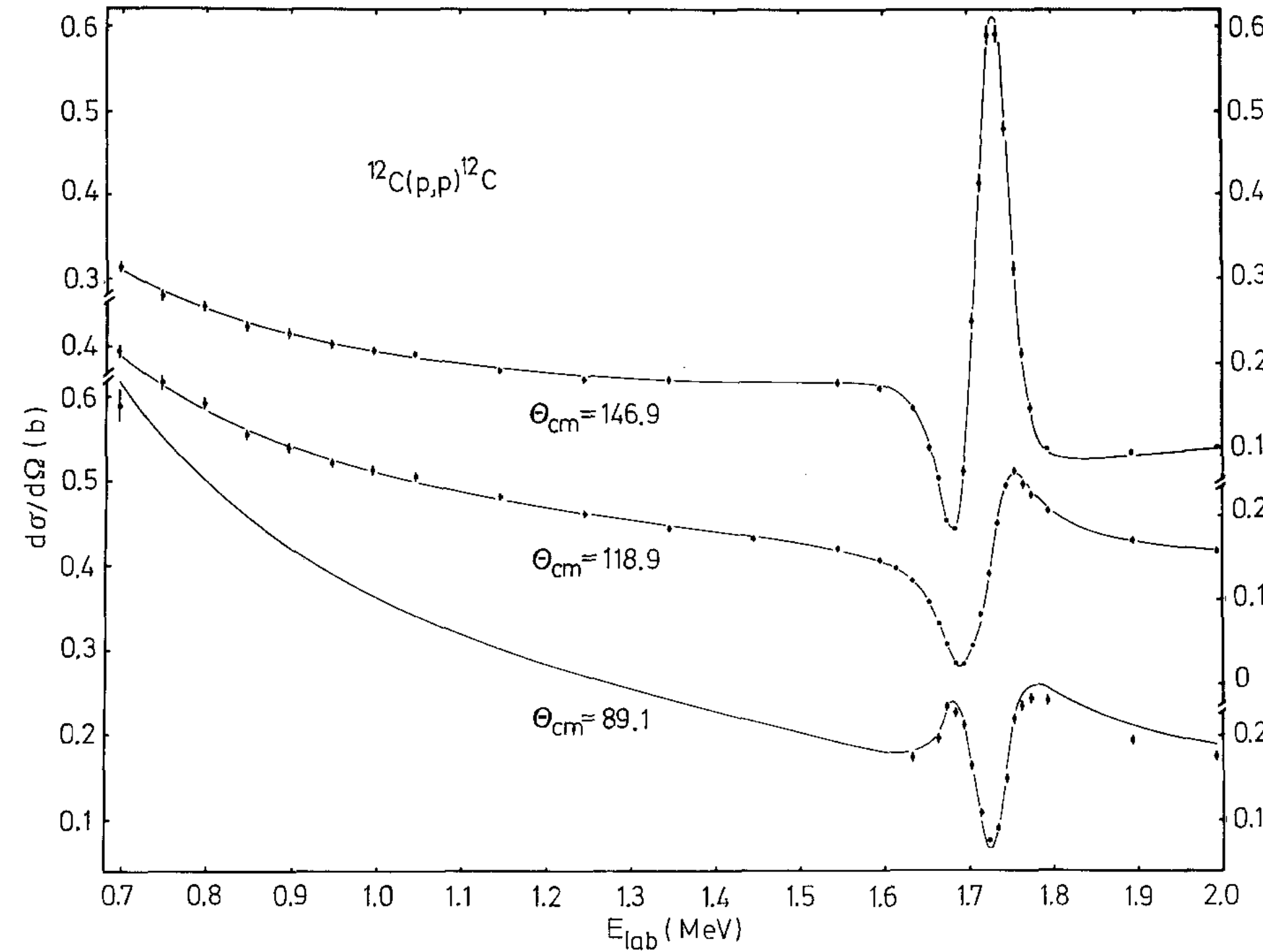
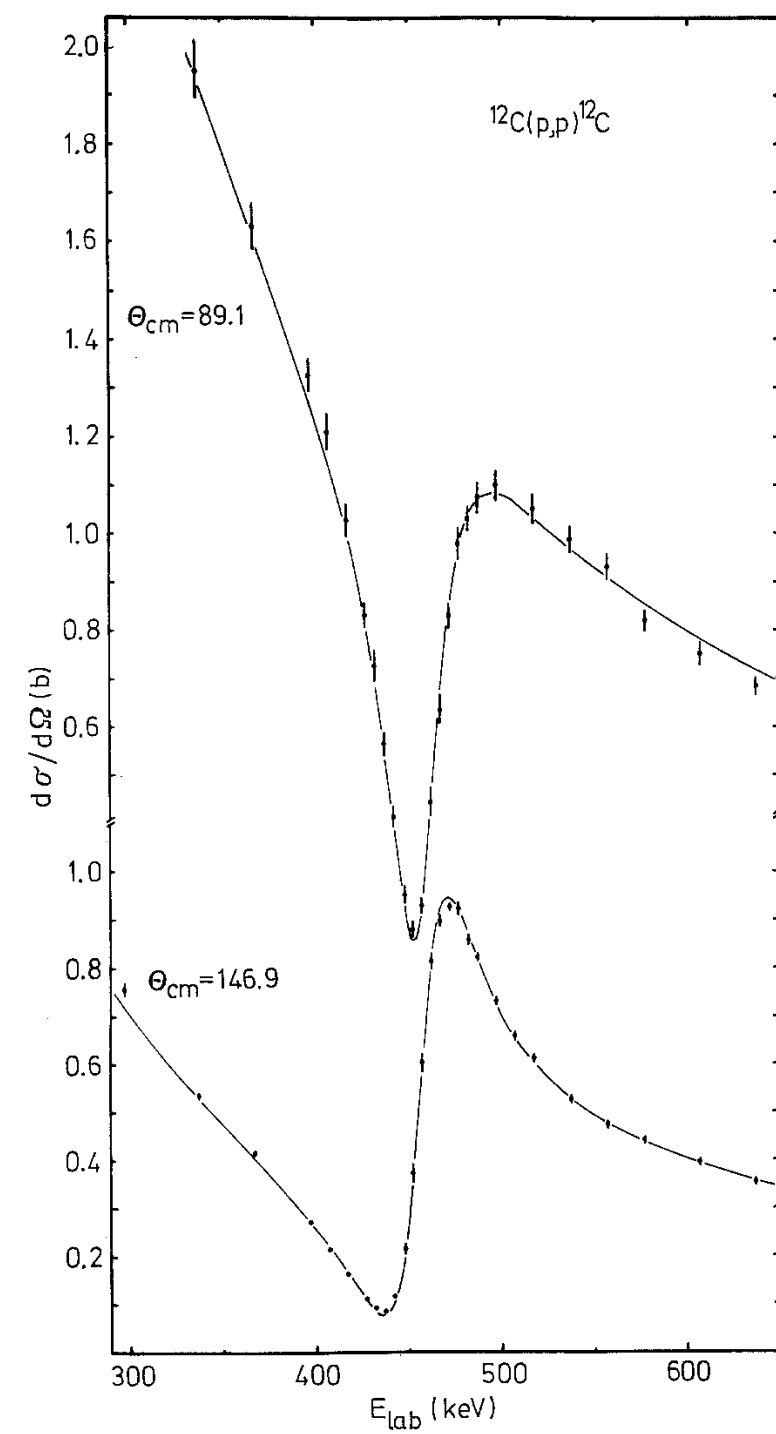
低エネルギー反核子散乱実験による 反核子-陽子（原子核）間相互作用の研究

藤岡 宏之（東京科学大学）

低エネルギー核子原子核散乱

p+¹²C

n+²⁷Al

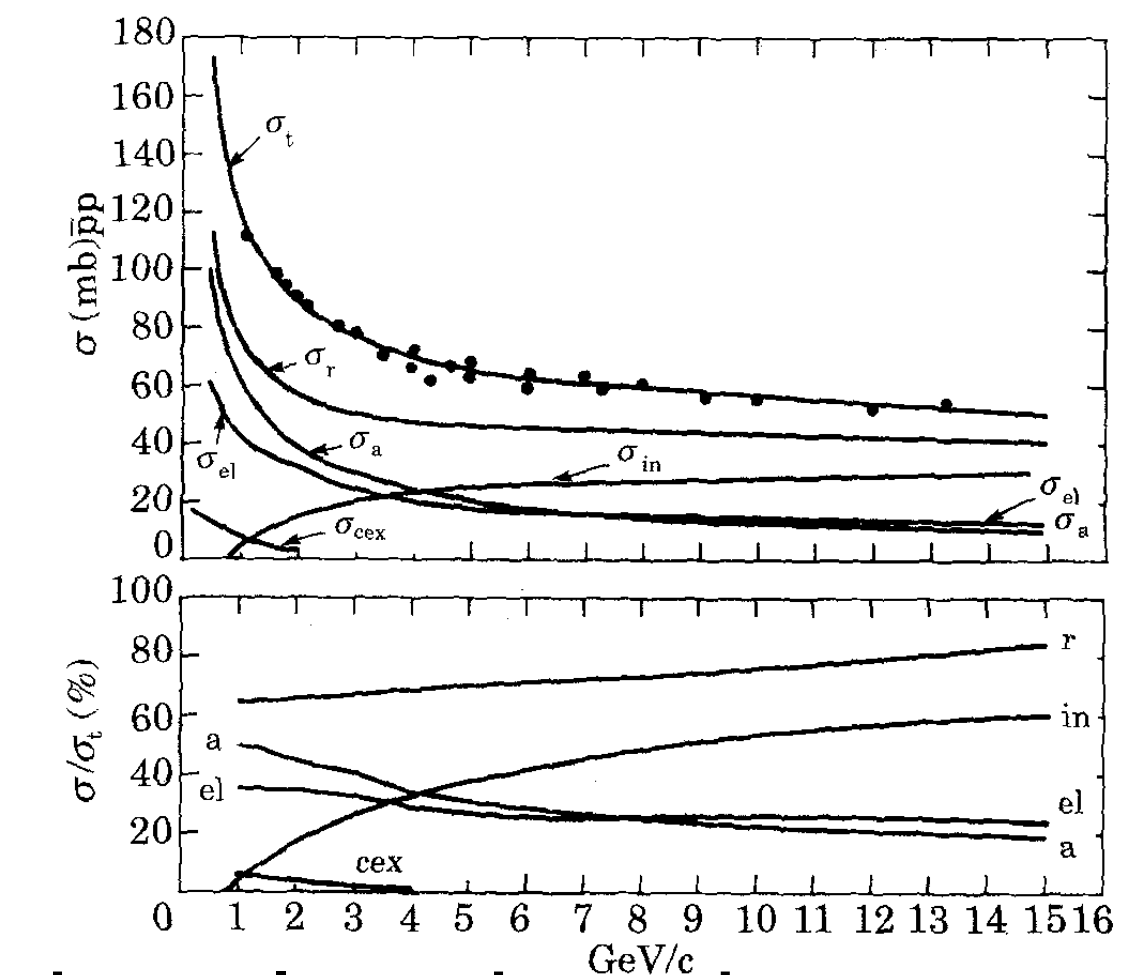
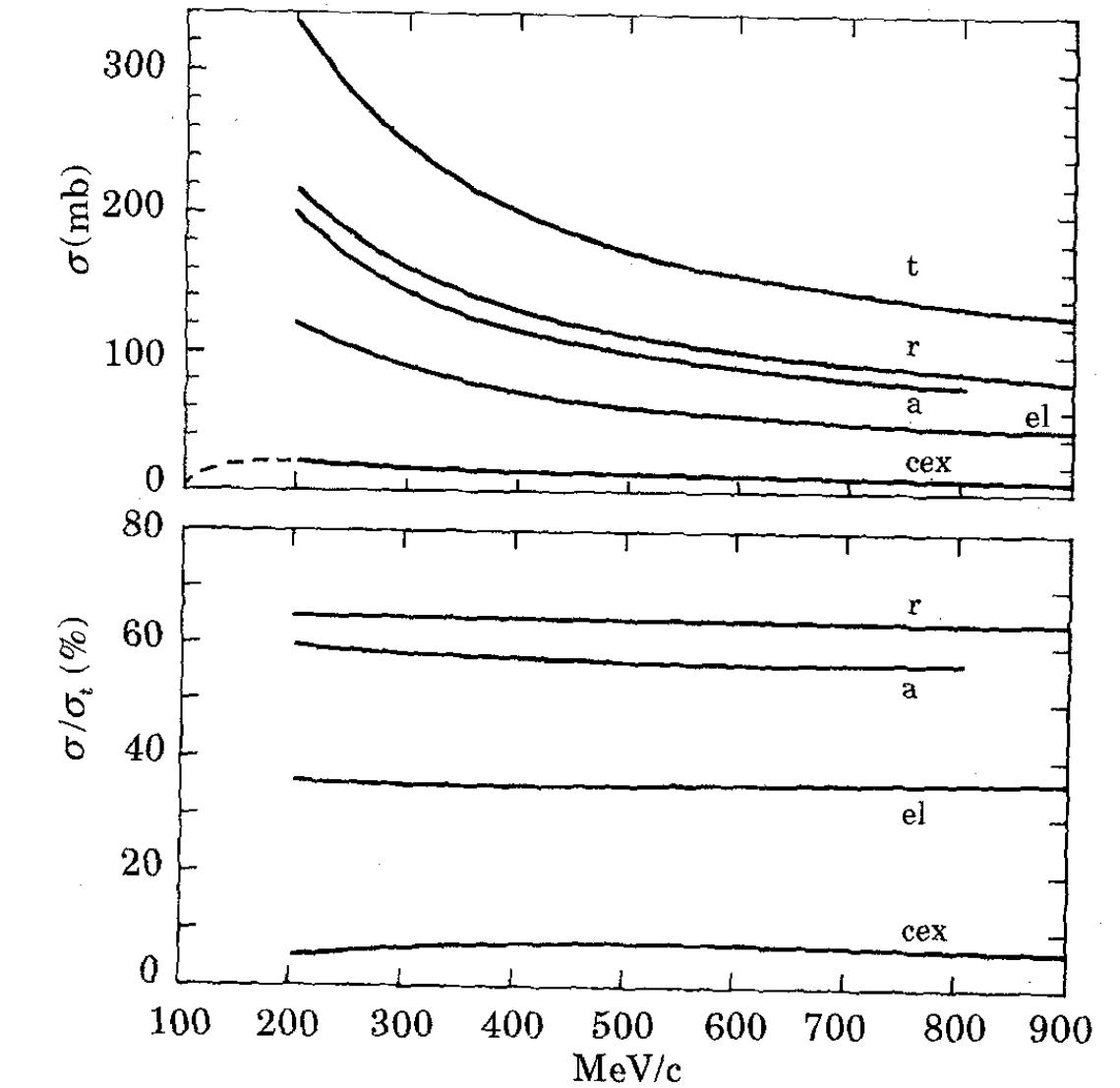


H. Meyer, G. Plattner, and I. Sick, Z. Phys. A279, 41 (1976)

JENDL-5

低エネルギー核子散乱と反核子散乱の違い

- 弾性散乱以外の反応：対消滅 ($\bar{N}N \rightarrow \text{multiple } \pi\text{'s etc.}$) が支配的
 - ▷ cf. 荷電交換反応 $\bar{p}p \rightarrow \bar{n}n$ の反応閾値は 98 MeV/c (5.1 MeV)
- 強い吸収： $|V_0| \lesssim |W_0| \sim \mathcal{O}(10^2) \text{ MeV}$
- 断面積のエネルギー依存性は単調：狭い共鳴は存在しない



G. Bendiscioli and D. Kharzeev,
Riv. Nuovo Cimento 17, 1 (1994)

- **We propose to construct a new beamline at CERN-AD for antineutrons with unprecedented low energies ($p=9\text{MeV}/c$, $E=40\text{keV}$)**
- **Physics cases:**
 - ▷ antineutron-proton ($\bar{n}p$) scattering \Rightarrow isospin-1 $N\bar{N}$ interaction
 - ▷ antineutron-nucleus ($\bar{n}A$) scattering \Rightarrow antineutron-nucleus interaction
- **References:**
 - ▷ A. Filippi, HF, T. Higuchi, L. Venturelli, arXiv:2503.06972 [nucl-ex]
 - ▷ C. Amsler *et al.*, Letter of Intent, CERN-SPSC-2025-010, SPSC-I-261 (May 2025)
 - ▷ HF and T. Higuchi, Prog. Theor. Exp. Phys. 2026, 023C01 (2026)

antineutron–proton system

antineutron–nucleus system

cross-section measurements: $\sigma_{el}, \sigma_{ann}, \sigma_{tot}$

scattering theory (s-wave)

$$\ell = R \cdot p < \hbar/2$$

$R \sim (\text{nuclear size}) < 10 \text{ fm}$
 $p \sim 9 \text{ MeV}/c$

$$\sigma_{el} \approx 4\pi |a|^2 (1 - 2a_1 k)$$

$$\sigma_{ann} \approx \frac{4\pi}{k} a_1 - 8\pi a_1^2$$

**low-energy is the key
for the evaluation of
scattering lengths!**

BSM physics

hadron physics

scattering length: $a_{\bar{n}p}$

cf. antiproton-proton scattering,
protonium (antiproton-proton bound system)

comparison

$N\bar{N}$ interaction models

scattering length: $a_{\bar{n}A}$

antineutron-nucleus
optical potential

$$U(r) = V(r) - iW(r)$$

cf. antiproton-nucleus scattering,
antiprotonic atom spectroscopy

Fermi pseudopotential for
ultracold antineutrons

$$U_{\bar{n}} = \frac{2\pi\hbar^2}{m} N \frac{A+1}{A} a_{\bar{n}A}$$

input

"ultracold" $< 200 \text{ neV}$

n - \bar{n} oscillation search

- **The ASACUSA experiment at CERN-AD plans to measure antiproton-nucleus cross sections at 100 keV (~ 14 MeV/c) in near future.**
- **Physics cases:**
 - ▷ antiproton-nucleus ($\bar{p}A$) scattering \Rightarrow antiproton-nucleus interaction
 - ▷ prospect: antiproton-proton ($\bar{p}p$) scattering using carbon and CH₂ targets
- **References:**
 - ▷ H. Aghai-Khozani et al., Nucl. Phys. A 970, 366 (2018) @ 5.3 MeV
 - ▷ H. Aghai-Khozani et al., Nucl. Phys. A 1009, 122170 (2021) @ 125 keV

- One-boson-exchange models

- ▷ $V_{NN} = V_{\pi} + V_{2\pi} + V_{\eta} + V_{\rho} + V_{\omega} + \dots$

↓ G-parity transformation

- $V_{N\bar{N}} = -V_{\pi} + V_{2\pi} + V_{\eta} + V_{\rho} - V_{\omega} + \dots$

- ▷ The short-range part is replaced by an annihilation potential $V_0 + iW_0$

- NN Paris potential → N \bar{N} Paris potential

- Dover-Richard, Kohno-Weise, ... : Woods-Saxon-type annihilation potential

- Partial Wave Analysis [PRC 86 (2012) 044003]

- Chiral EFT [up to N³LO, JHEP 07(2017) 078]

- no Lattice QCD calculation

- All these approaches rely on experimental data, that are more than three decades old.

$N\bar{N}$ optical potential and phase shift

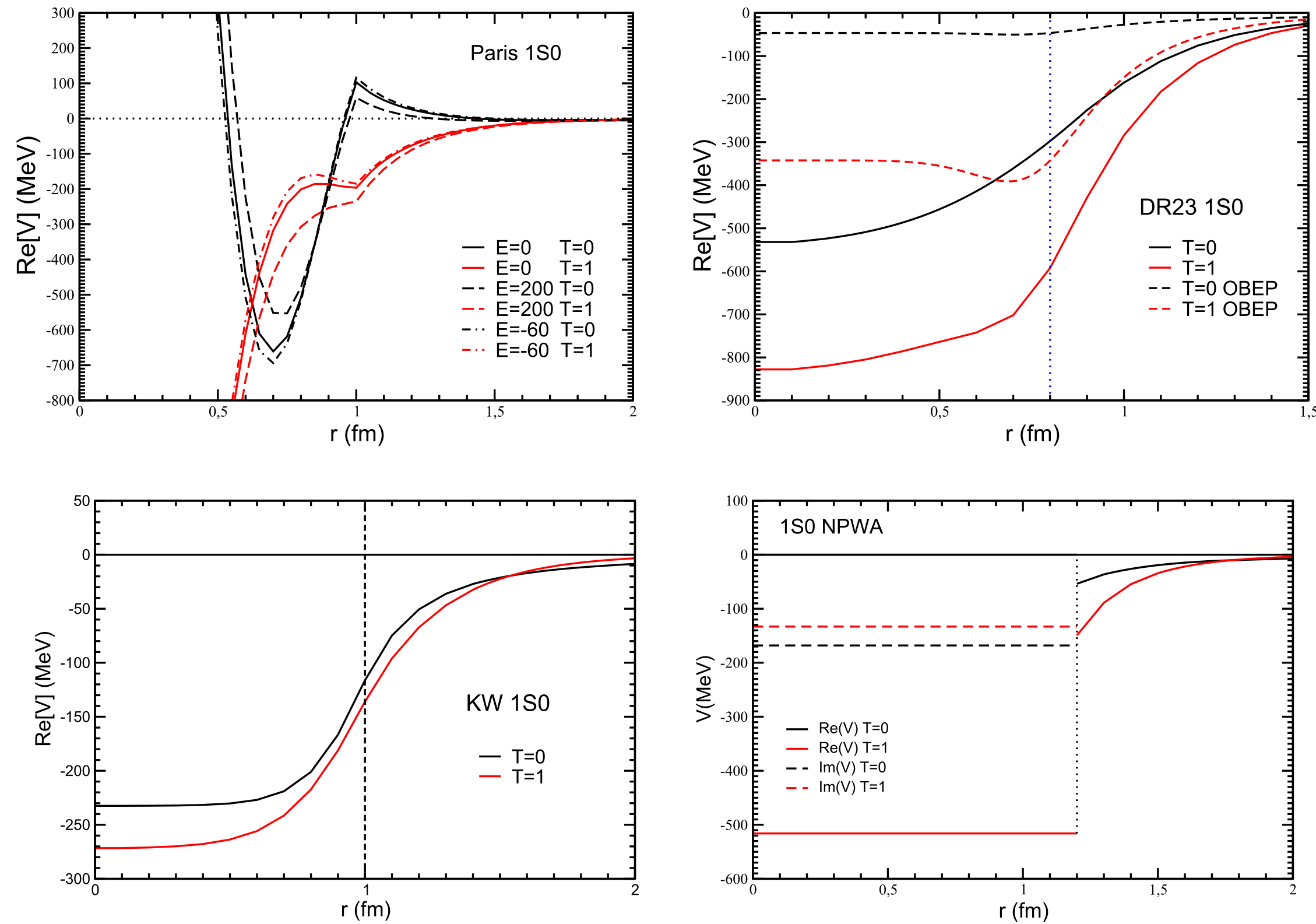


Fig. 15 Real parts of 1S_0 potentials for both isospins (T)

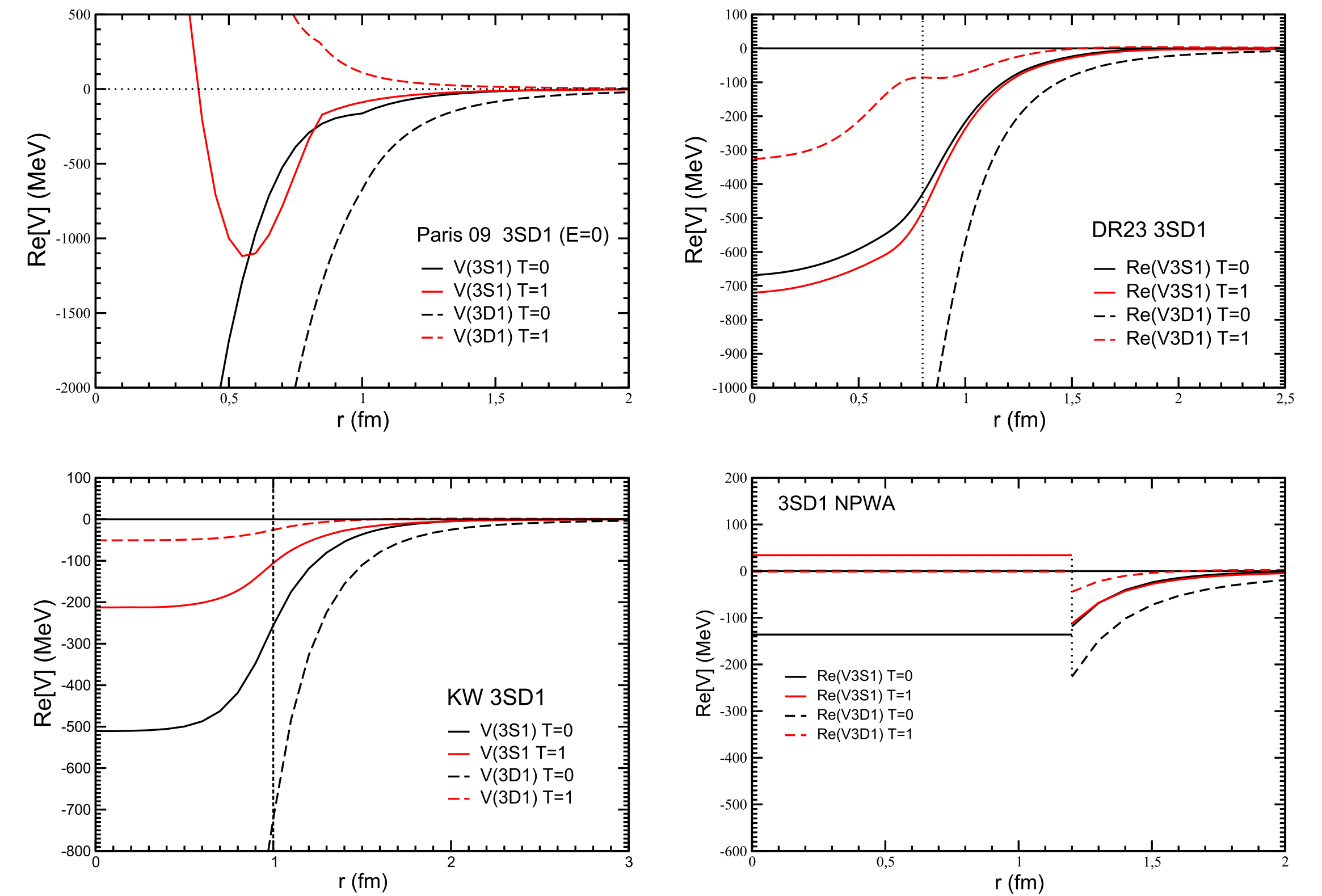


Fig. 16 Real parts of 3S_1 and 3D_1 potentials for both isospins (T)

$N\bar{N}$ optical potential and phase shift

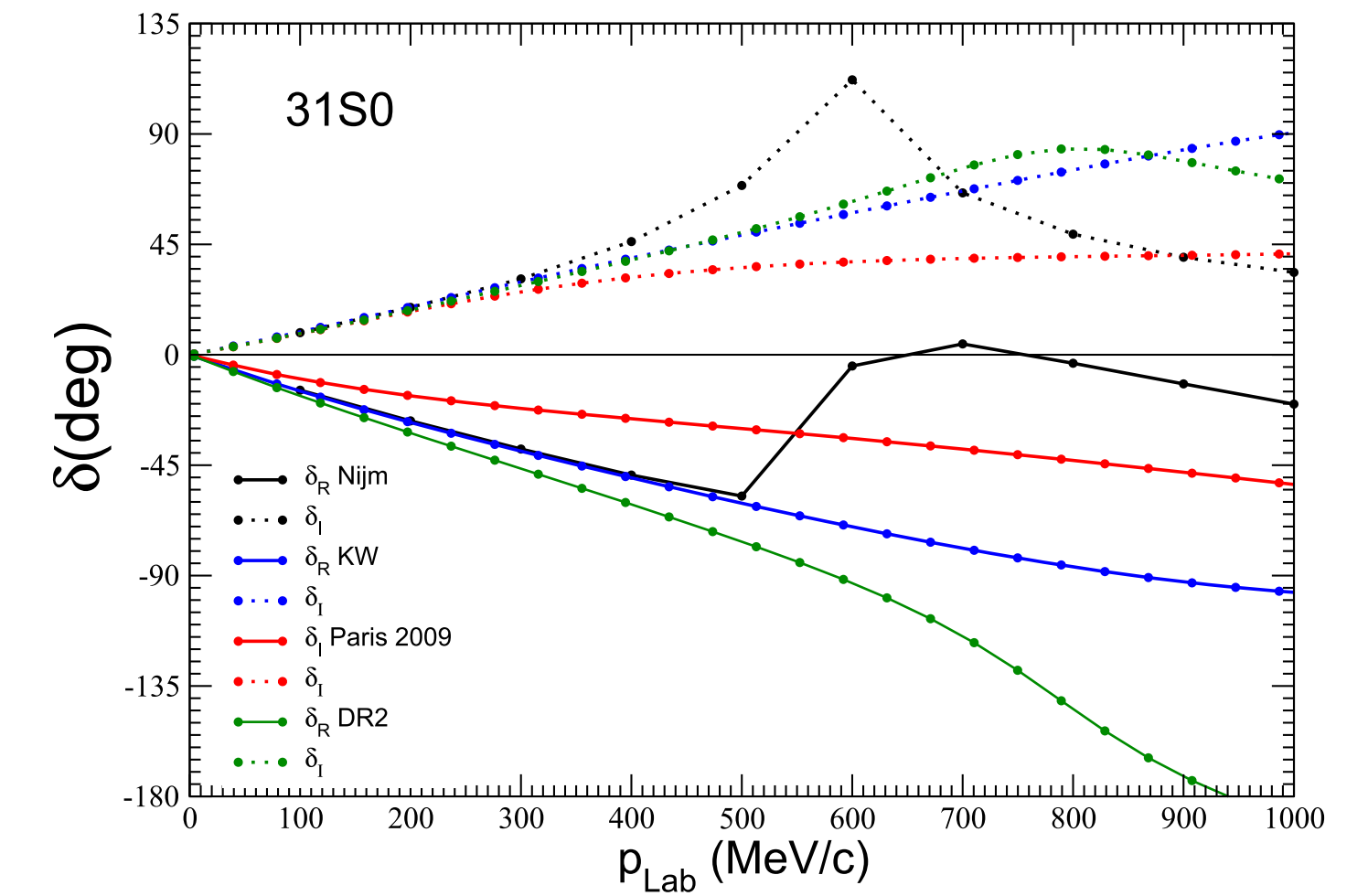
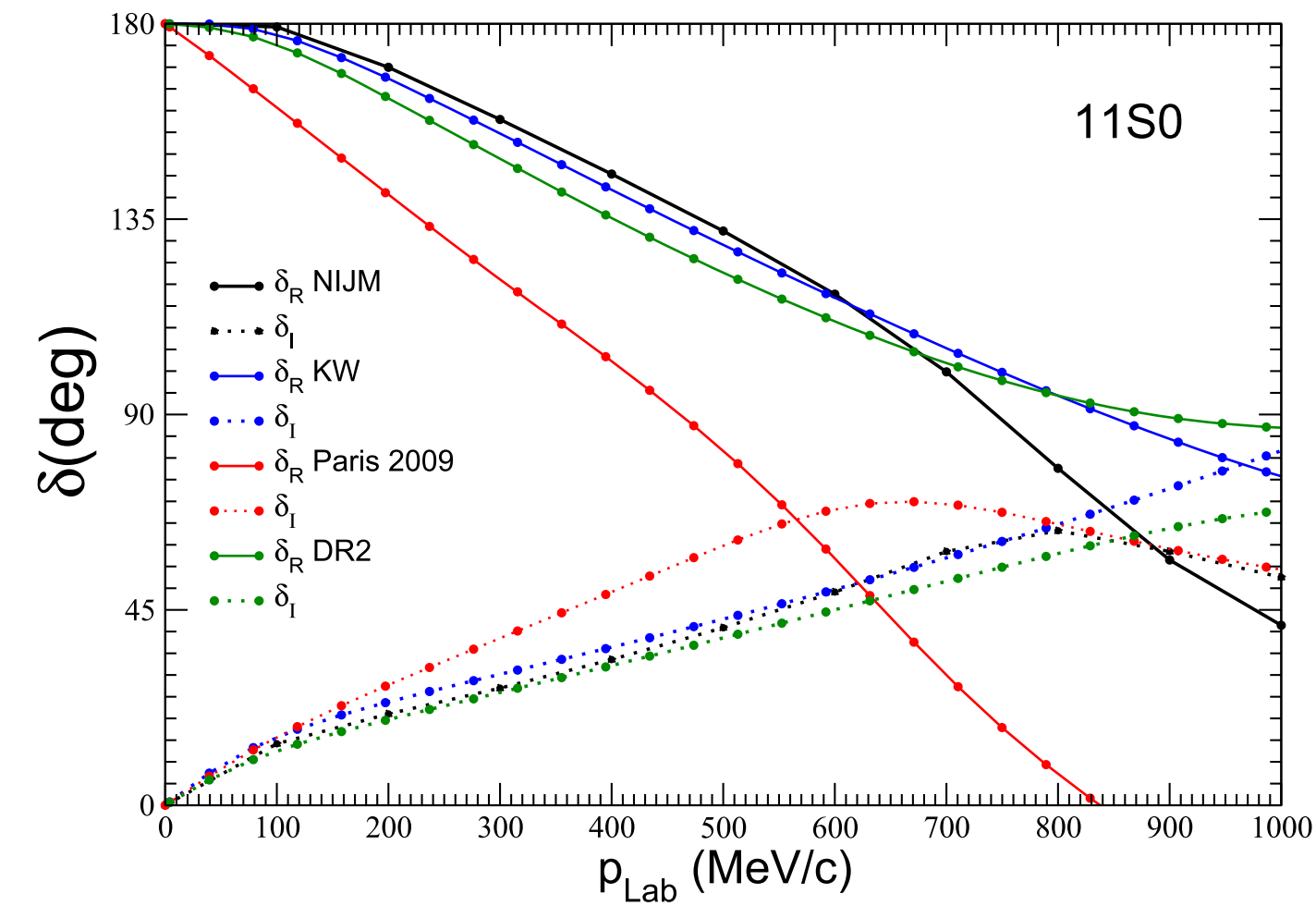
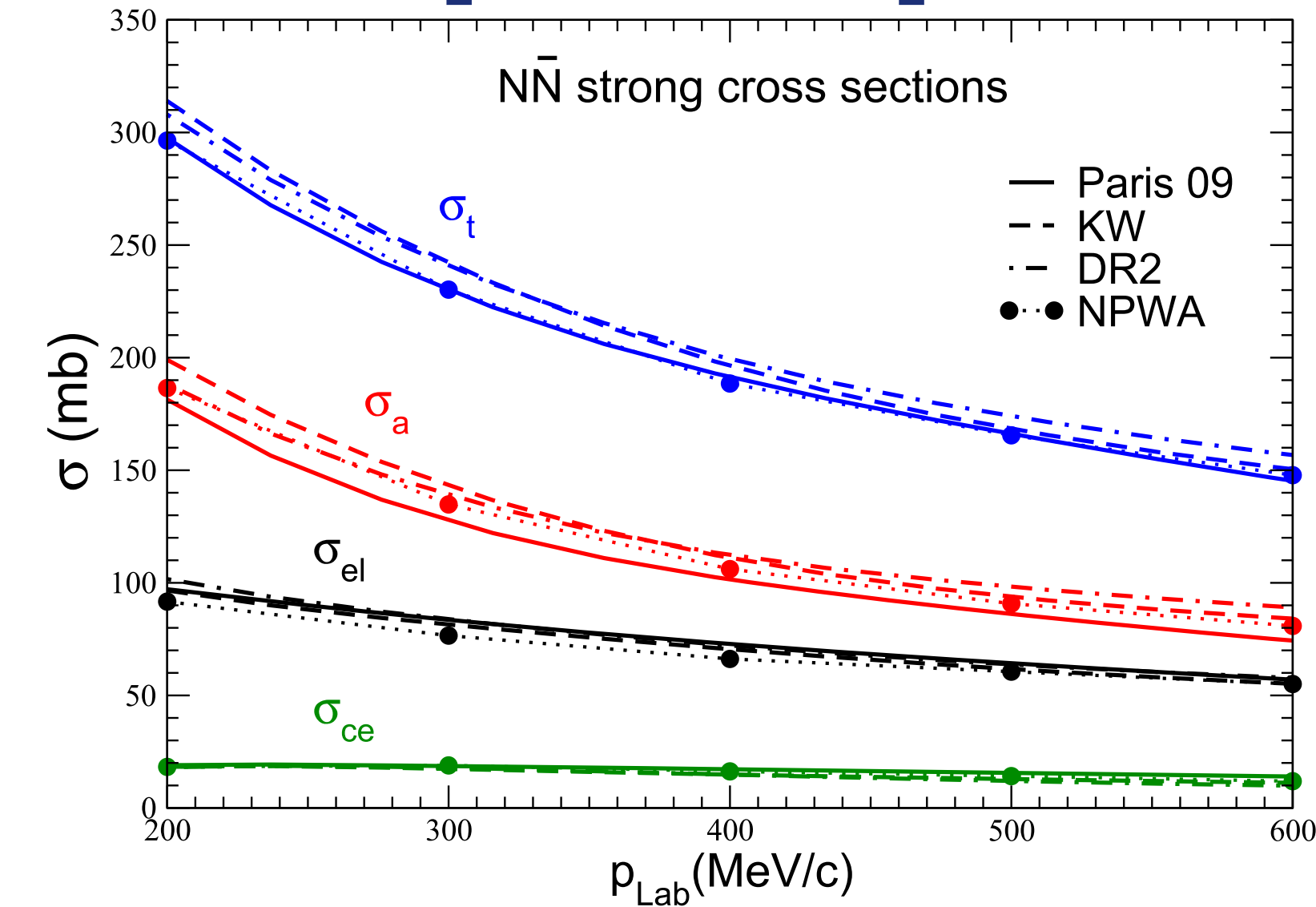
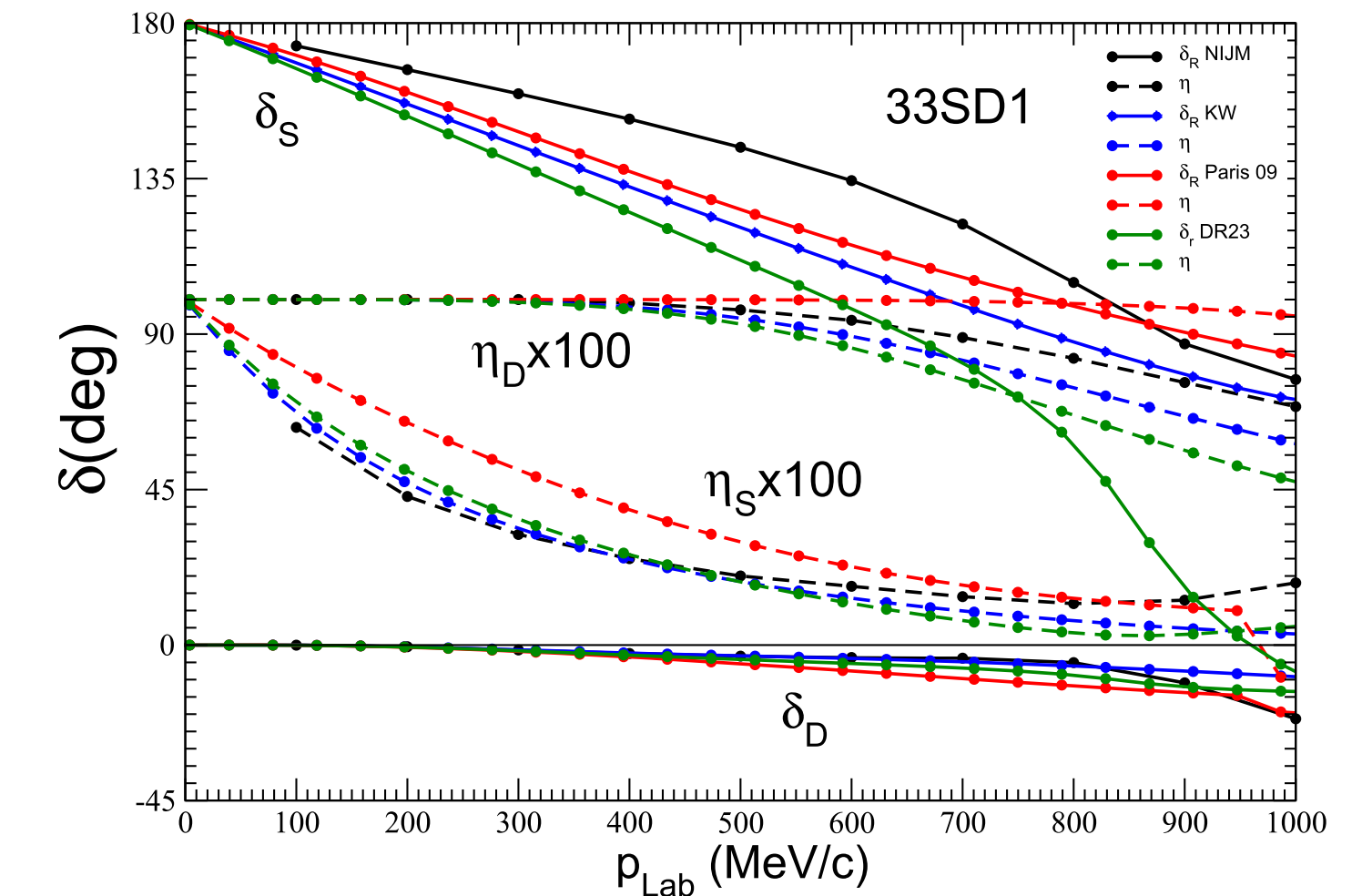
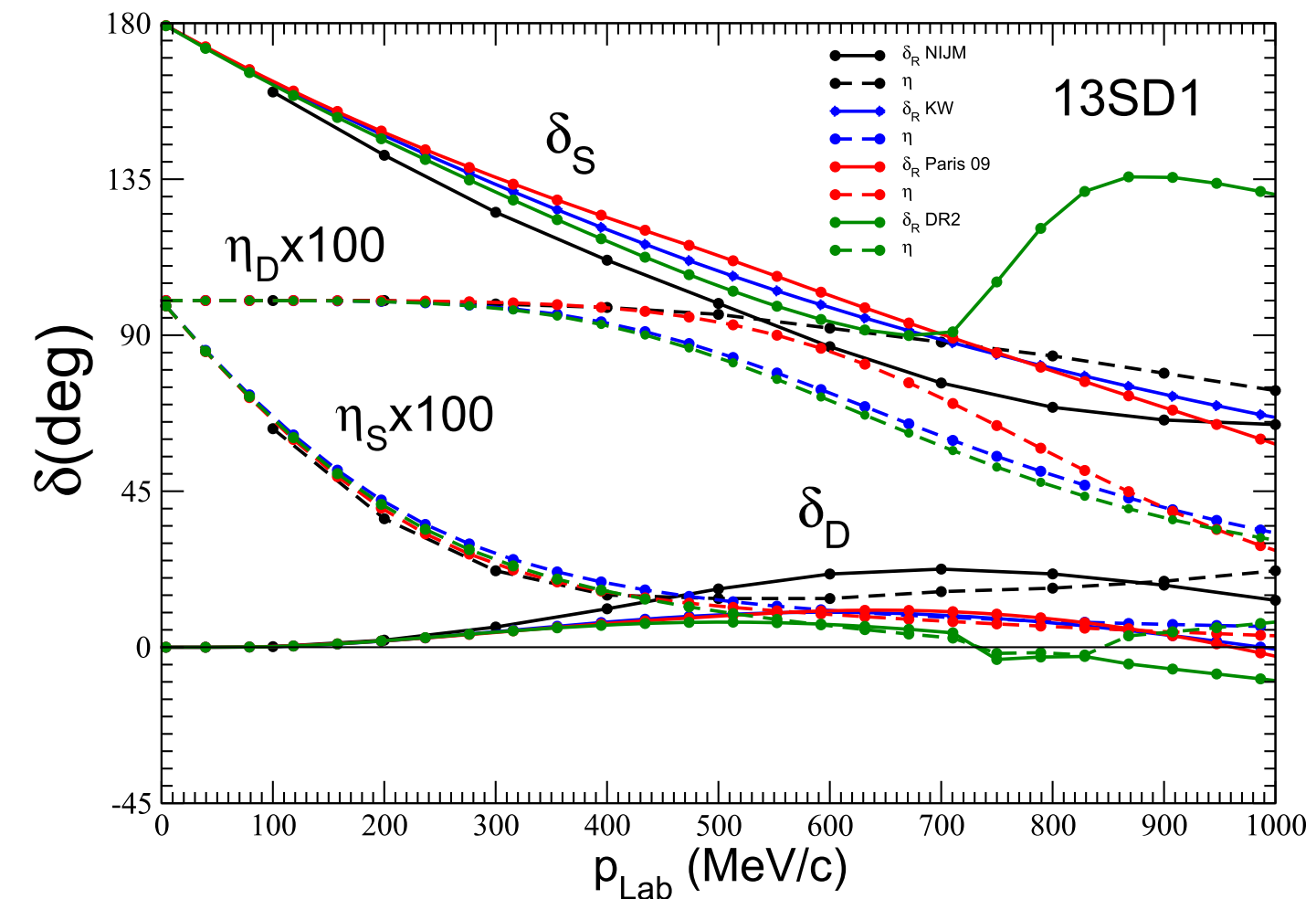


Table 2 S-wave $\bar{N}N$ low energy parameters (in fm) for the considered optical models: Jülich results are taken from Table 3 of Ref. [12], KW and DR2 from [20], Paris 2009 have been recomputed and are in agreement with [46]. The values of Nijmegen are obtained by extrapolating the phase shifts from Figs. 2 and 3

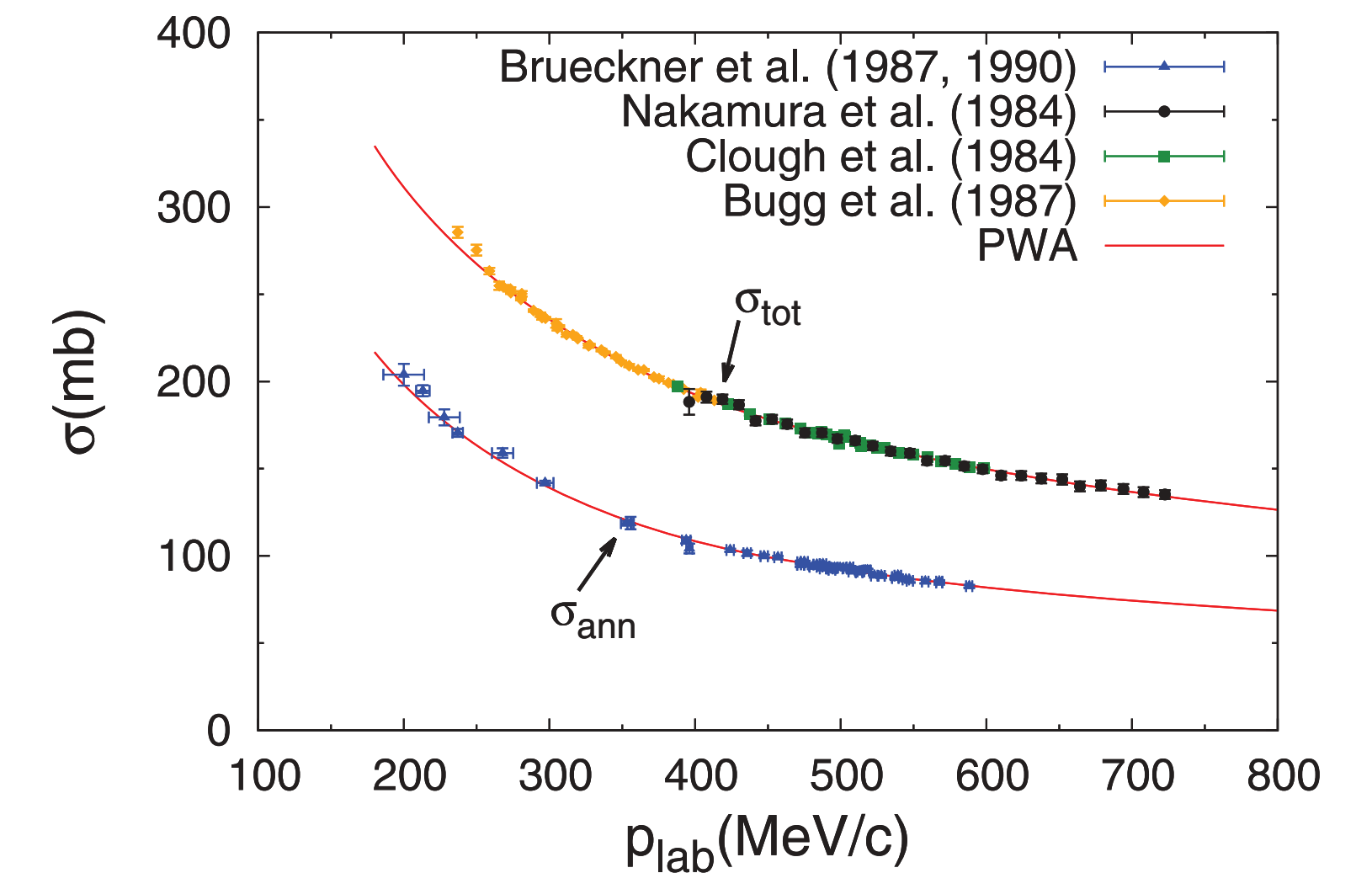
T = 0	a_0 $^{11}S_0$	r_0	a_0 $^{13}SD_1$	r_0
Nijm*	-0.17 -1.01i	-6.9-2.9 i	-	-
Jülich	-0.21 -1.23i	-	1.42-0.88i	-
Paris 09	1.27 -1.18i	-0.53+0.14i	1.20-0.80i	-
KW	-0.03-1.35i	-4.7-7.9i	1.23-0.77i	-
DR2	0.10 -1.07i	-11-6.2i	1.28-0.78i	-
T = 1	a_0 $^{31}S_0$	r_0	a_0 $^{33}SD_1$	r_0
Nijm*	1.02 -0.60i	0.7-1.2i	-	-
Jülich	1.05 -0.58i	-	0.44-0.96i	-
Paris 09	0.76 -0.56i	0.9-3.9i	0.61-0.44i	-
KW	1.07 -0.62i	0.7-1.9i	0.78-0.80i	-
DR2	1.20 -0.57i	0.6-1.6i	0.89-0.71i	-



- for elastic ($p\bar{p} \rightarrow p\bar{p}$) and charge-exchange ($p\bar{p} \rightarrow n\bar{n}$) scattering data

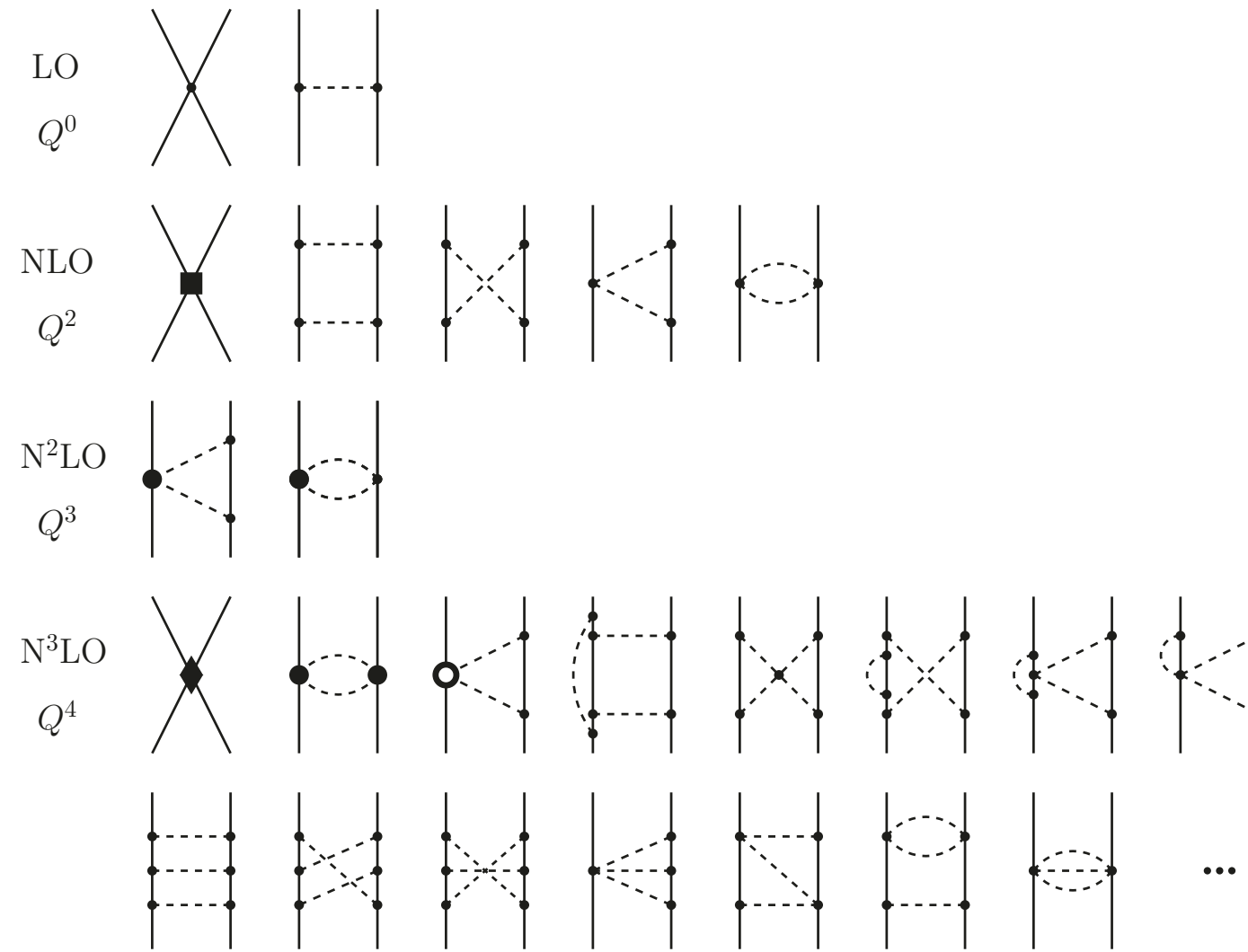
TABLE III. Reference table of antiproton-proton scattering data with $p_{\text{lab}} \leq 923 \text{ MeV}/c$. The asterisks in the leftmost column indicate the data sets that were not included in Ref. [23], because the data are more recent or because the values of the data points were not available. The meanings of the superscripts in the heading and the comments in the rightmost column are given at the end of the table.

p_{lab} (MeV/c)	No., ^a type ^b	χ_{min}^2	Norm error (%) ^v	Predicted norm ^c	Rejected ^d	Ref.	Comment
119.0–923.0	50 σ_{ce}	46.5	4	1.058	$\leq 385.0, \# = 8; 468.0$	[45]	k,m
176.8–396.1	5 σ_{ann}	9.4	4.4	0.949	176.8	[46]	
181.0	46 $d\sigma_{\text{el}}$	–	5	–	All	[47,48]	j,l,o
183.0	13 $d\sigma_{\text{ce}}$	13.3	5	1.002	0.940, –0.170, –0.574	[49]	
194.8	19 $d\sigma_{\text{el}}$	–	4	–	All	[50]	f,i,o
200.0–588.2	48 σ_{ann}	52.5	2.2	0.989		[46,51]	
221.9–413.2	45 σ_{tot}	55.3	∞	0.961	221.9, 229.6, 254.9, 260.8, 280.3, 289.1, 394.2, Norm	[52]	
				•			
				•			
				•			
875.0*	9 $D_{yy,\text{ce}}$	5.1	–	–		[74,88]	q
875.0*	5 $K_{yy,\text{ce}}$	5.9	–	–		[89]	q
886.0	34 $d\sigma_{\text{el}}$	–	∞	–	All	[71]	h,l
886.0	34 $A_{y,\text{el}}$	34.1	4.5	1.023		[70,71]	
886.0	1 $D_{yy,\text{el}}$	1.5	–	–		[79]	q
910.0	19 $d\sigma_{\text{el}}$	–	∞	–	All	[90]	f,g
910.0	21 $A_{y,\text{el}}$	12.9	5	0.990		[90]	



D. Zhou and R. G. E. Timmermans,
Phys. Rev. C 86, 044003 (2012)

Chiral Effective Field Theory



N²LO: X.-W. Kang, J. Haidenbauer, U.-G. Meißner, JHEP 02, 113 (2014)

N³LO: L.-Y. Dai, J. Haidenbauer, U.-G. Meißner JHEP 07, 078 (2017)

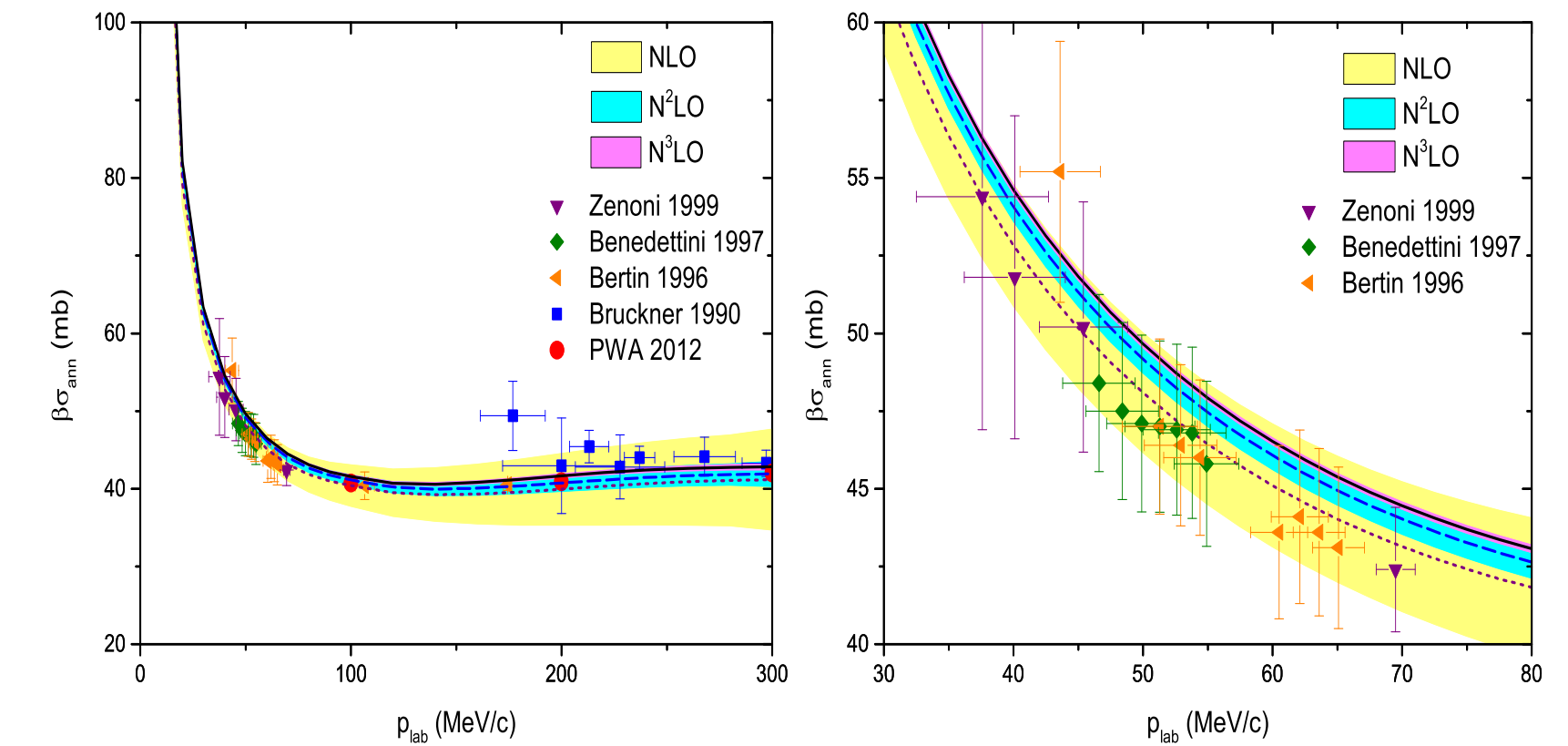
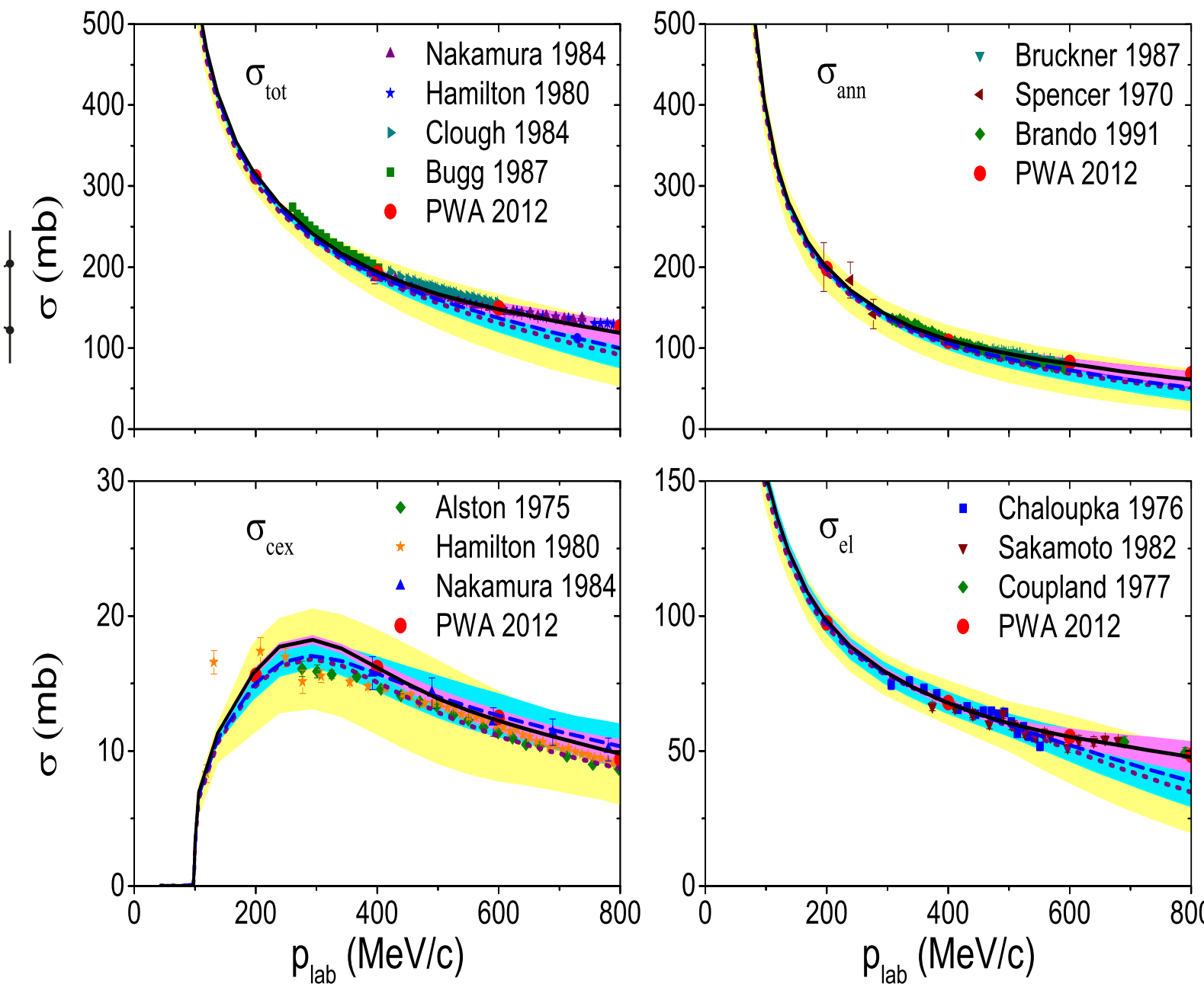


Figure 14. $\bar{p}p$ annihilation cross section multiplied by the velocity β of the incoming \bar{p} . Notations are described in the text. The results of the PWA [32] are indicated by circles. Data are taken from [104–107].

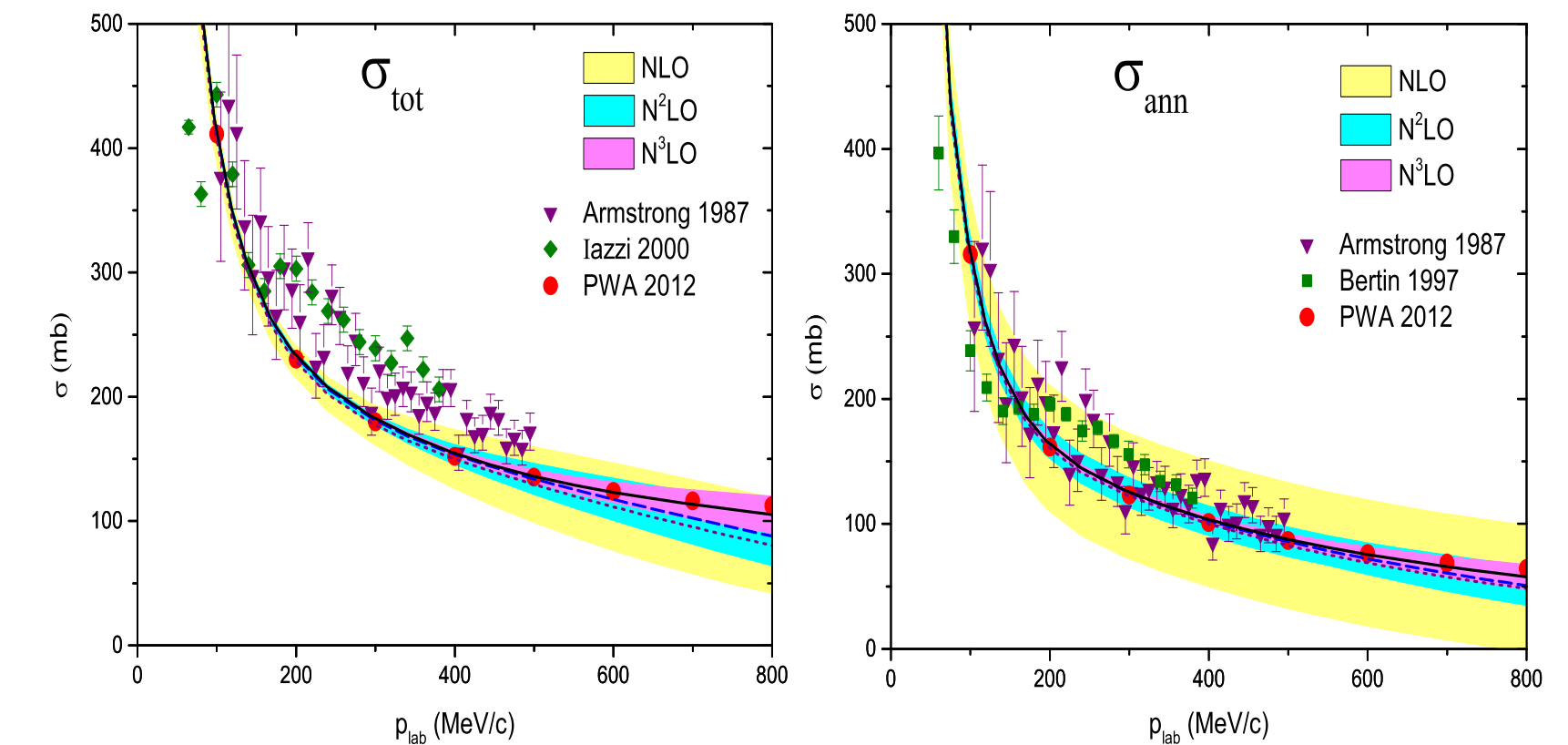
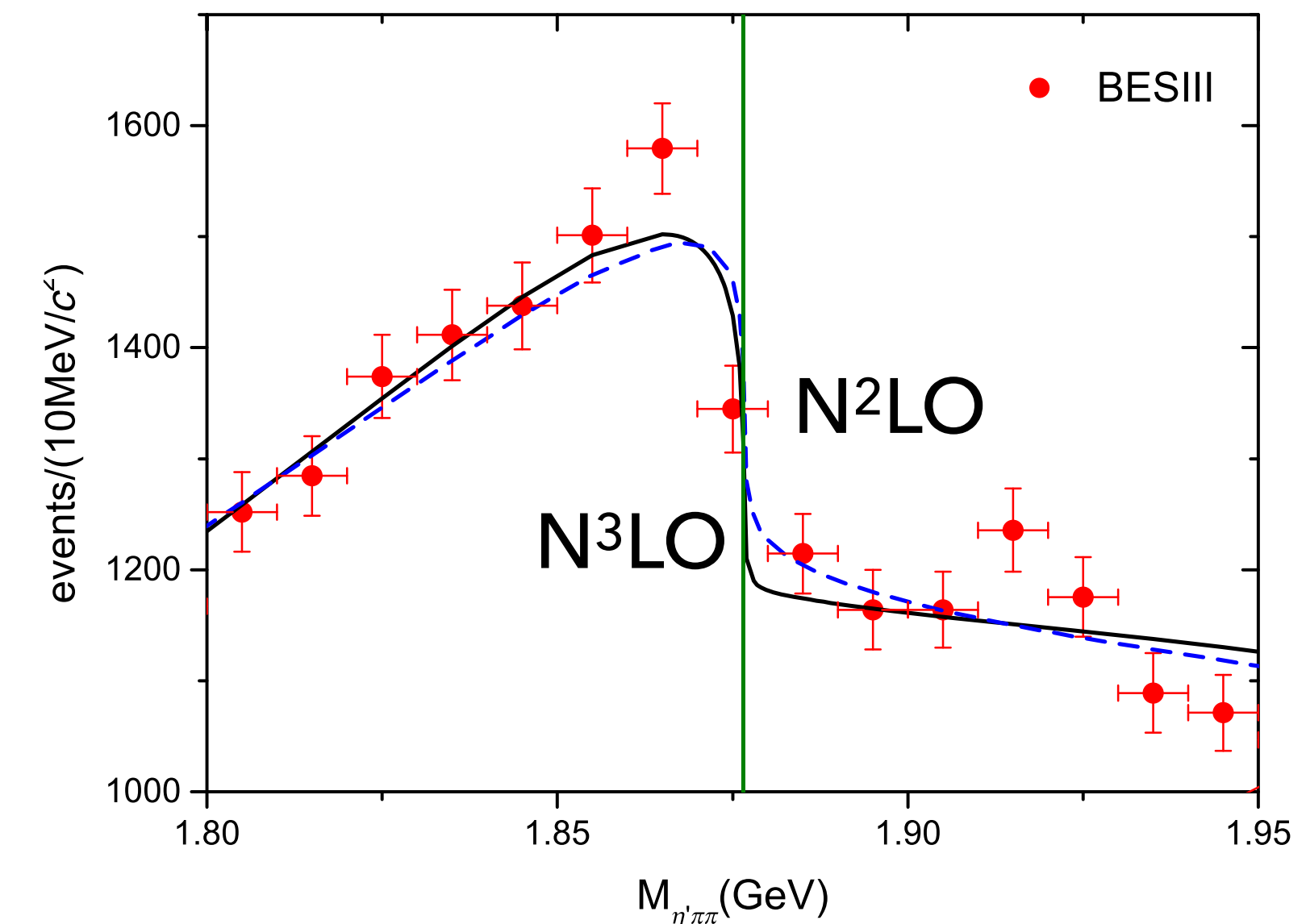
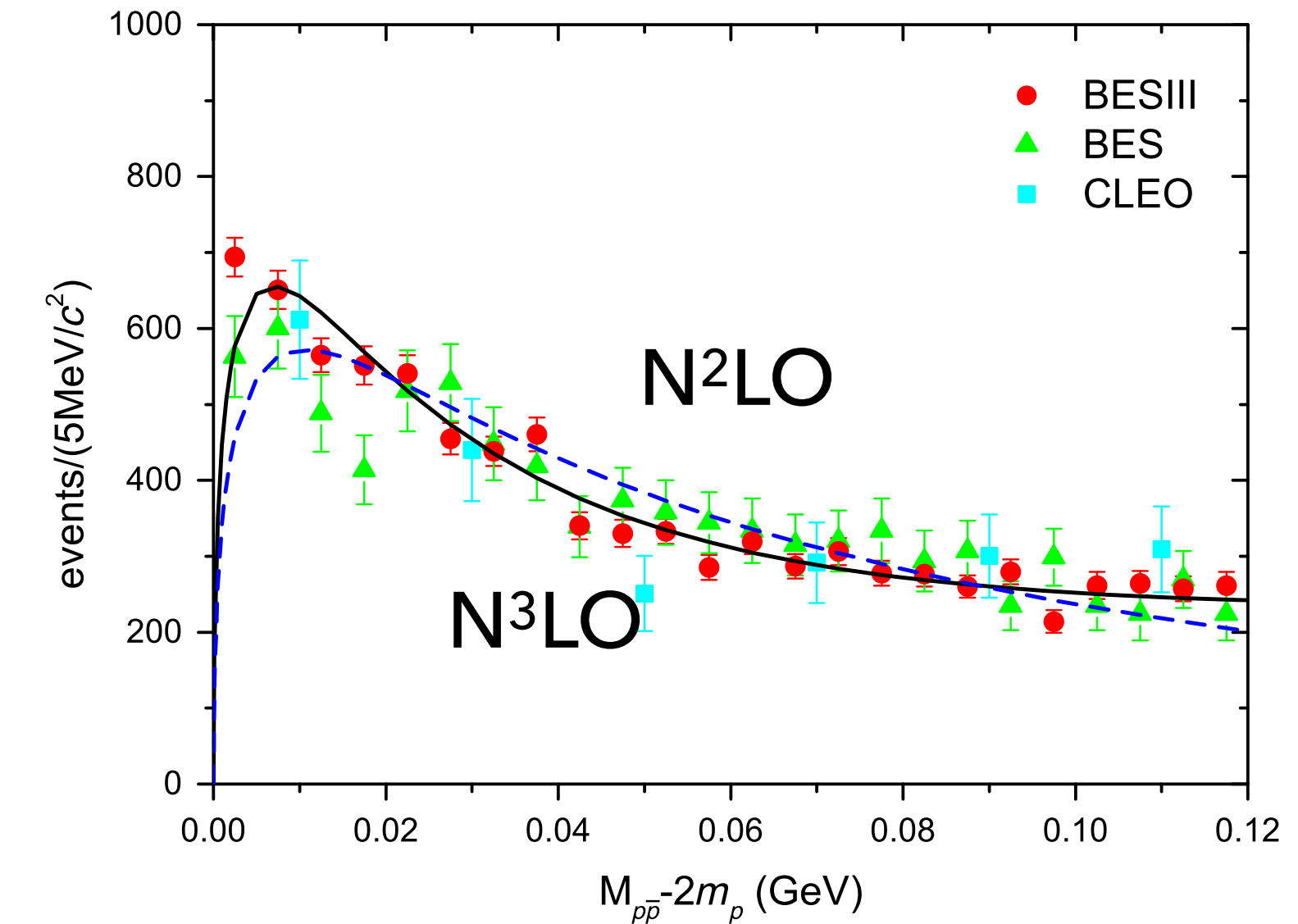
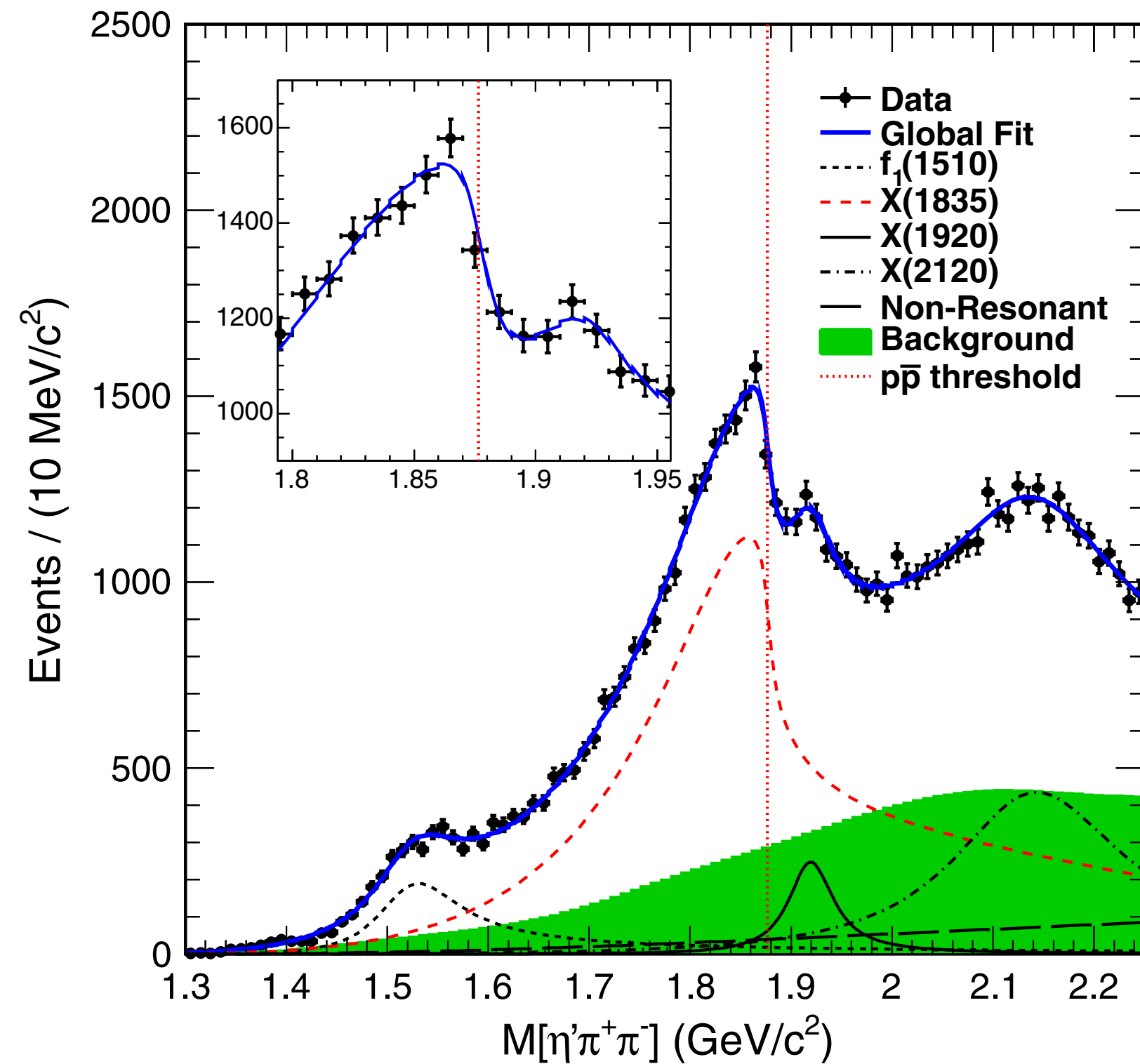


Figure 15. Total (σ_{tot}) and integrated annihilation (σ_{ann}) cross sections for $\bar{n}p$ scattering. Notations are described in the text. Data are taken from refs. [109–111].

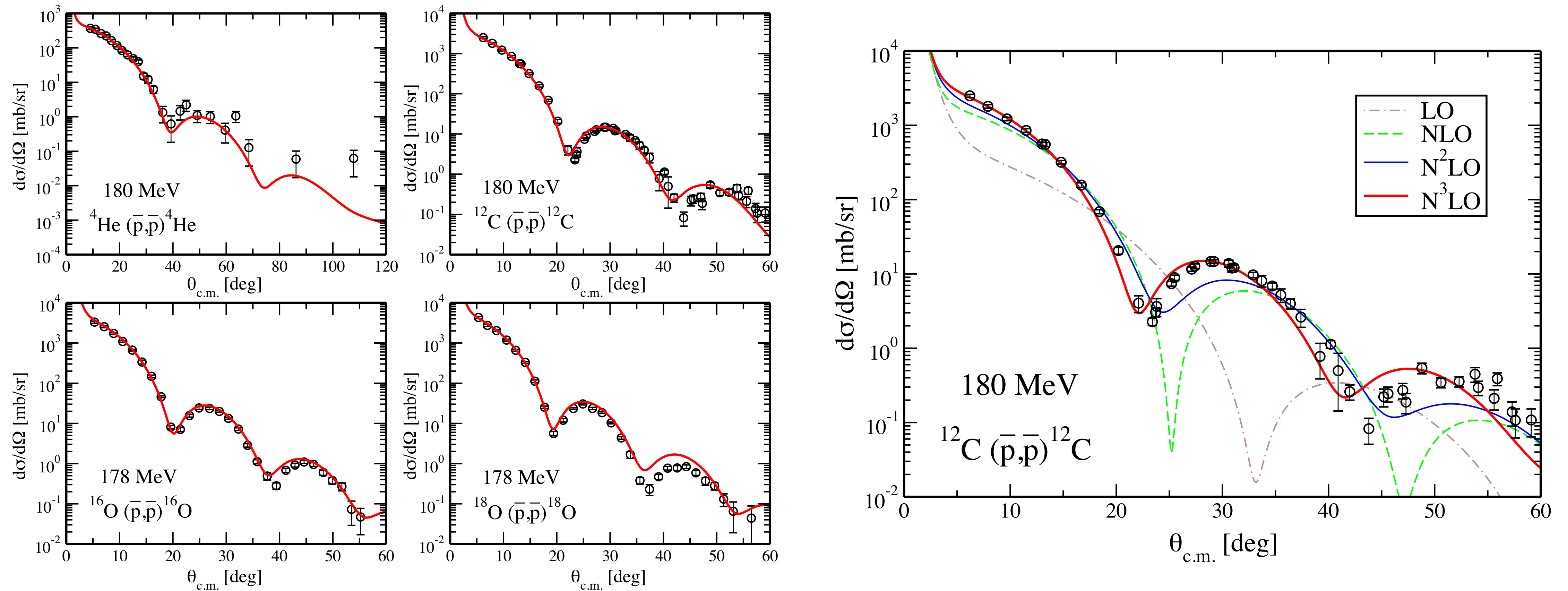
X(1835) or $p\bar{p}$ FSI in J/ψ decay?

$$J/\psi \rightarrow \gamma p\bar{p} \rightarrow \gamma \eta' \pi^+ \pi^-$$



Elastic scattering from Chiral Forces

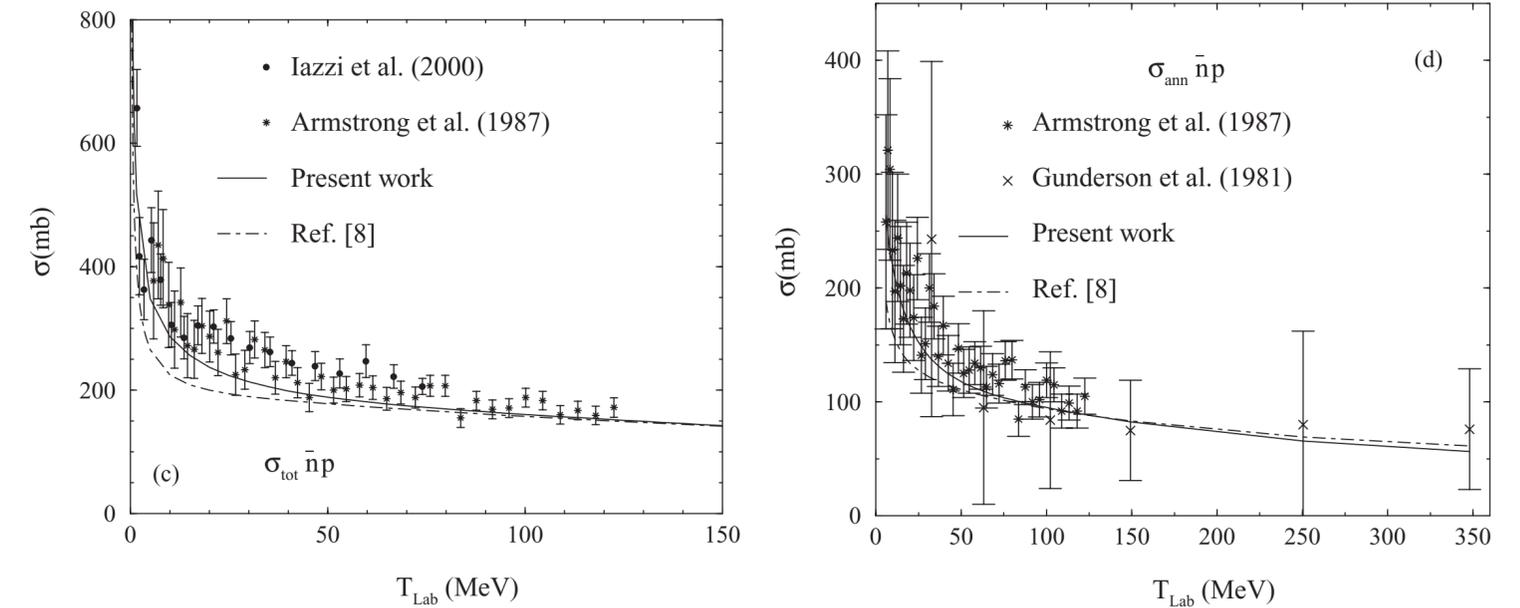
- microscopic optical potential, constructed with chiral $\bar{p}N$ forces
+ nuclear densities obtained from *ab initio* calculations (NN and 3N interactions)



M. Vorabbi, M. Gennari, P. Finelli, C. Giusti, P. Navrátil, Phys. Rev. Lett. 124, 12501 (2020)

Low-energy $\bar{n}p$ scattering

- purely in the isospin=1 channel
- only adopted in a recent work on the Paris potential updated in 2009.
- Many parameters (spin, isospin, partial wave) have to be fixed in each model.
- We propose a model-independent approach to determine scattering lengths by low-energy scattering measurements.



Paris '09: B. El-Bennich,^{1,2} M. Lacombe,¹ B. Loiseau, and S. Wycech, *Phys. Rev. C* 79, 054001 (2009)

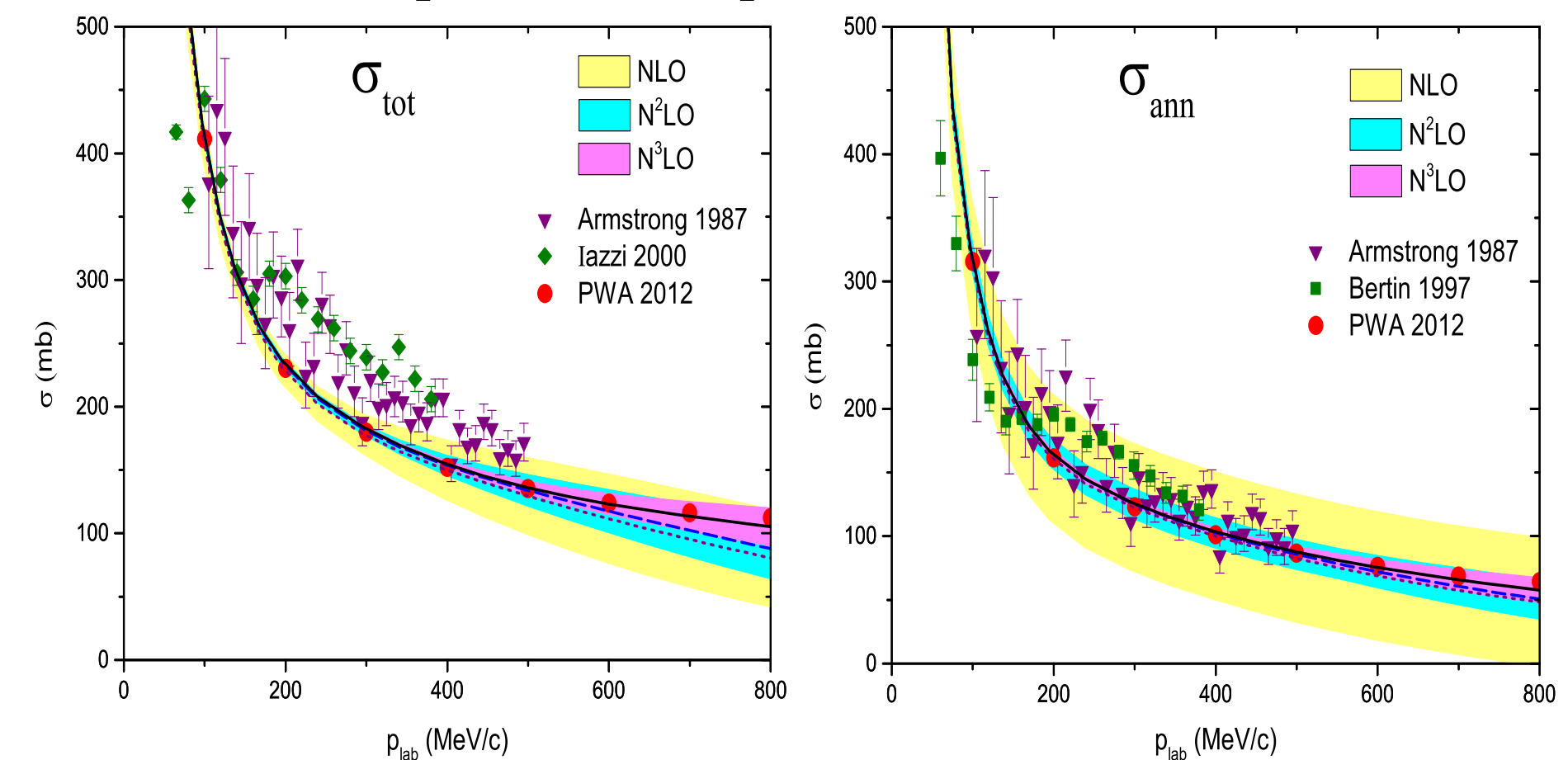


Figure 15. Total (σ_{tot}) and integrated annihilation (σ_{ann}) cross sections for $\bar{n}p$ scattering. Notations are described in the text. Data are taken from refs. [109–111].

Low-energy $\bar{n}p$ scattering

- Only S-wave scattering is important in case of $\hbar k = p_{\text{Lab}}/2 \lesssim 25 \text{ MeV}/c$
- scattering amplitude: $f_{\ell=0} = 1/(k \cot \delta - ik)$
 - ▷ $k \cot \delta \approx -1/a \equiv \alpha = \alpha_R - i\alpha_I$ ($\alpha_I > 0$) in the low-energy limit
 - ▷ scattering length: $a = a_R - ia_I$ ($a_I > 0$)

- elastic scattering cross section:
$$\sigma_{\text{el}} = \frac{4\pi}{\alpha_R^2 + (\alpha_I + k)^2} \approx 4\pi |a|^2 (1 - 2a_I k)$$

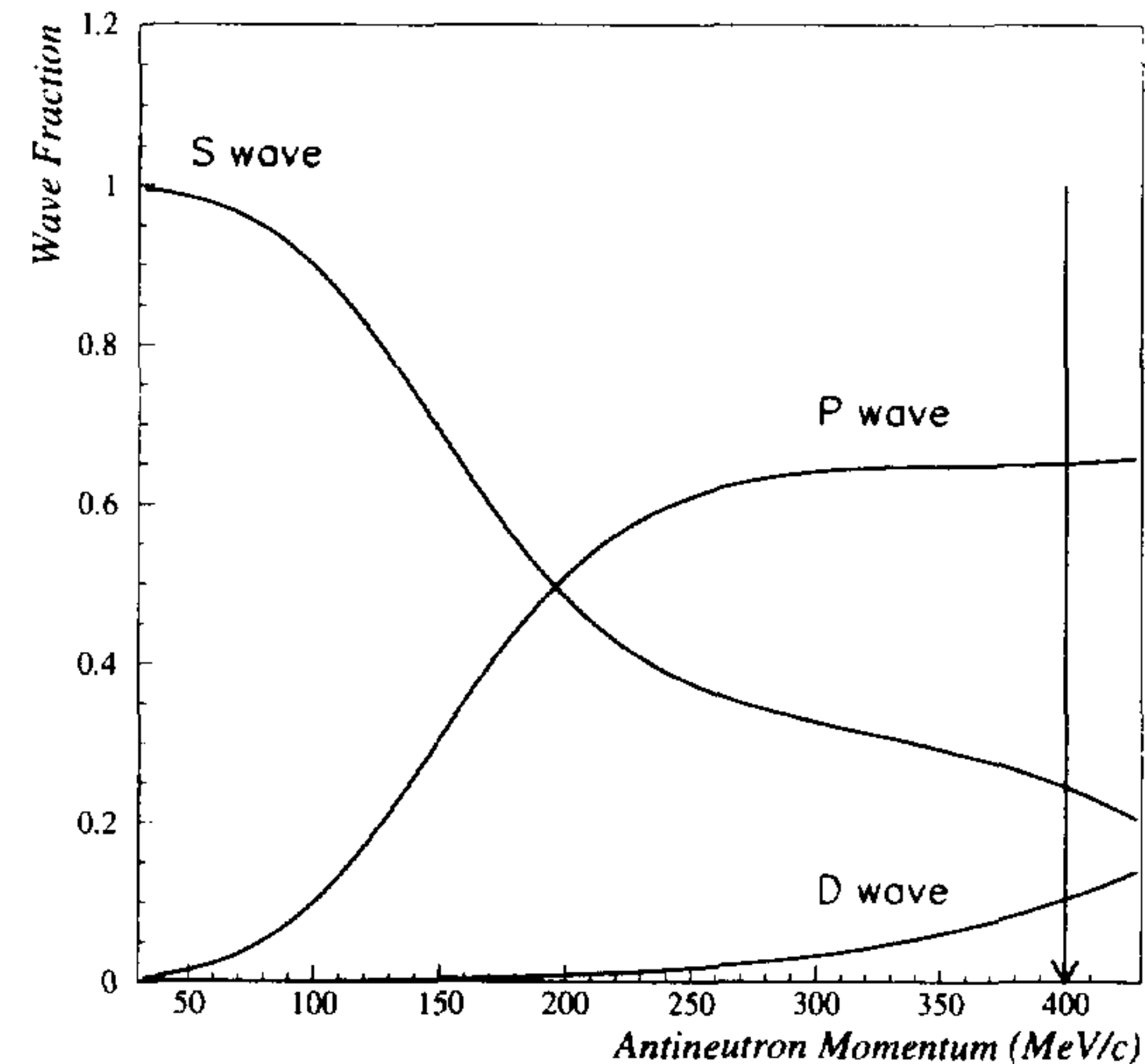
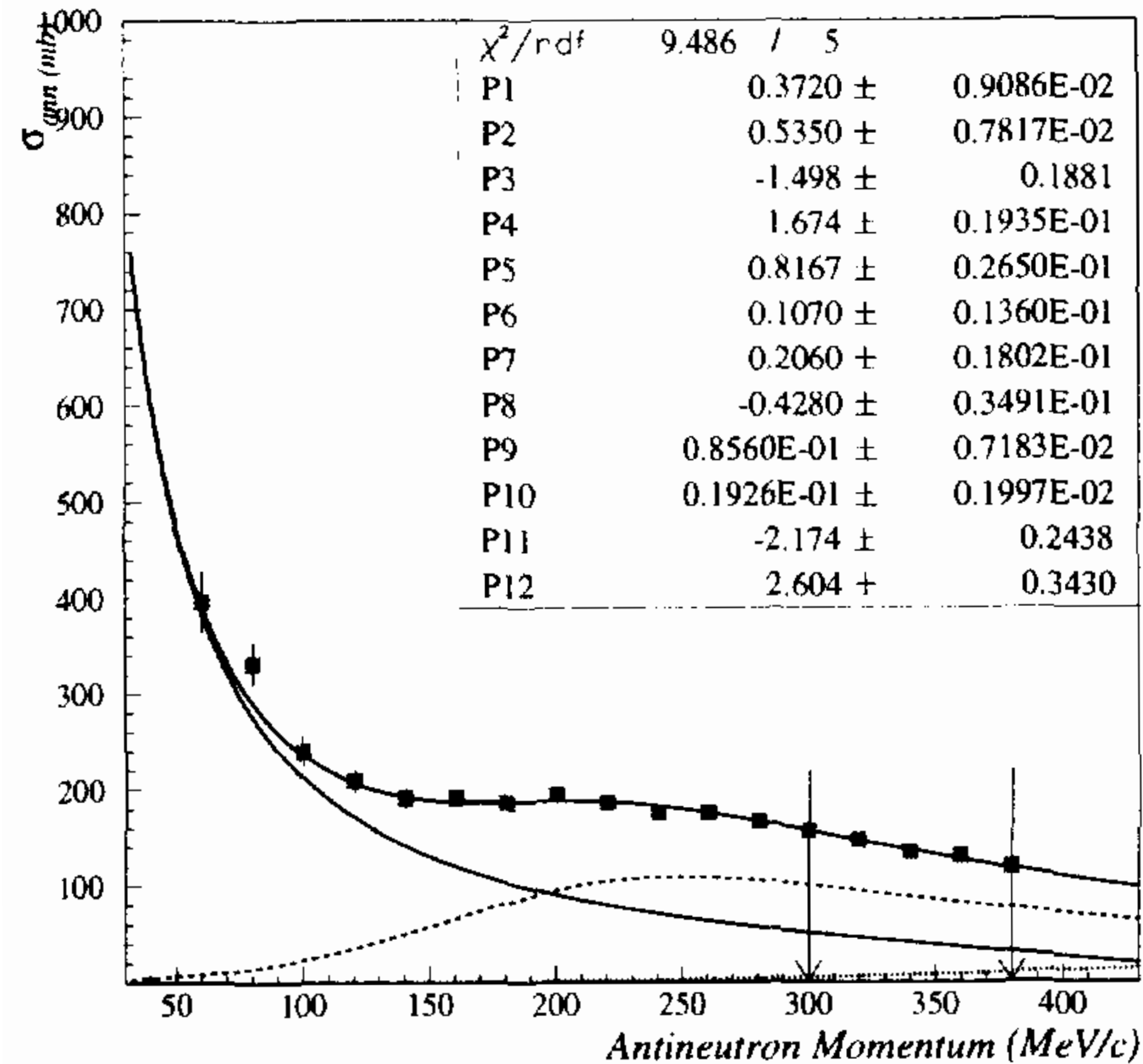
- annihilation cross section:
$$\sigma_{\text{ann}} = \frac{4\pi}{k} \frac{\alpha_I}{\alpha_R^2 + (\alpha_I + k)^2} \approx \frac{4\pi}{k} a_I - 8\pi a_I^2$$

proportional to $1/v$

$\bar{n}p$ annihilation at OBELIX

S, P and D-wave parameters from the fit of $\sigma_{ann}^{\bar{n}p}$ up to 400 MeV/c.

$a_1(fm)$	$r_1(fm)$	$b_1(fm^3)$	$R_1(fm)$	$c_1(fm^5)$	$\rho_1(fm)$	χ^2/n
$0.37 + i0.53$	$-1.5 + i1.67$	$0.82 + i0.11$	$0.21 - i0.43$	$0.086 + i0.019$	$-2.17 + i2.6$	9.5/5



A. Bertin et al., Nucl. Phys. B 56A (1997) 227c

Low-energy $\bar{p}p$ scattering (annihilation)

- Due to attractive Coulomb interaction
 - ▷ $\sigma \propto v^{-2}$ instead of $\sigma \propto v^{-1}$
 - ▷ p-wave doesn't vanish even when $E \rightarrow 0$
 - ▷ Coulomb-corrected scattering length a_{sc} can be deduced as follows:

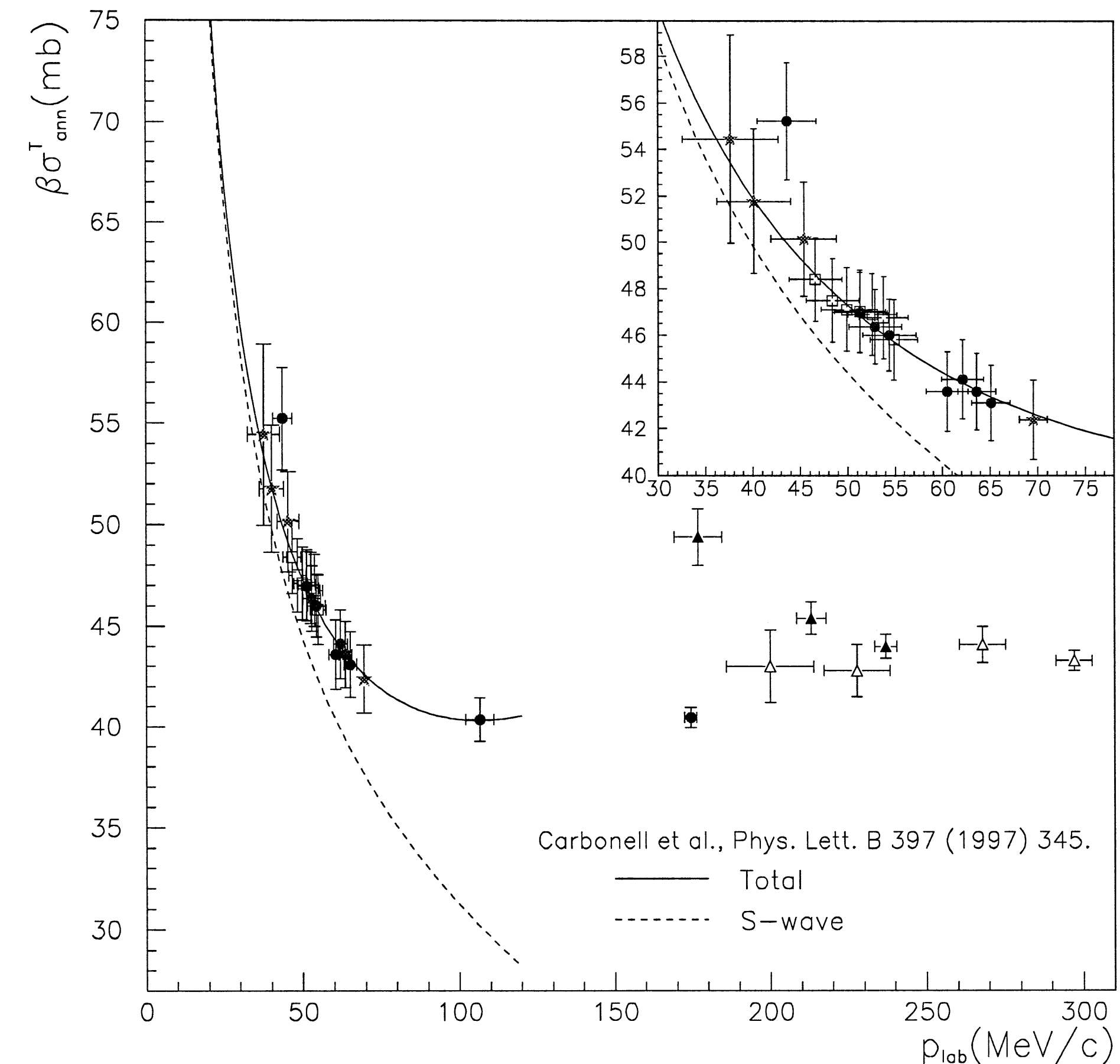
$$q^2 \sigma_{\text{ann}}^{\text{sc}} (\text{S-wave}) = \frac{8\pi^2}{1 - e^{2\pi\eta}} \frac{\text{Im}(-a_{sc}/B)}{|1 + iq w(\eta) a_{sc}|^2}, \quad (1)$$

where:

- $\eta = -1/qB$ is the dimensionless Coulomb parameter with B the $\bar{p}p$ Bohr radius;
- $w(x) = c_0^2(x) - 2ixh(x)$ is an auxiliary function with $qBw(\eta) \rightarrow 2\pi$ when $q \rightarrow 0$;
- c_0^2 and h are the usual functions in the Coulomb scattering theory

$$c_0^2(x) = \frac{2\pi x}{\exp(2\pi x) - 1};$$

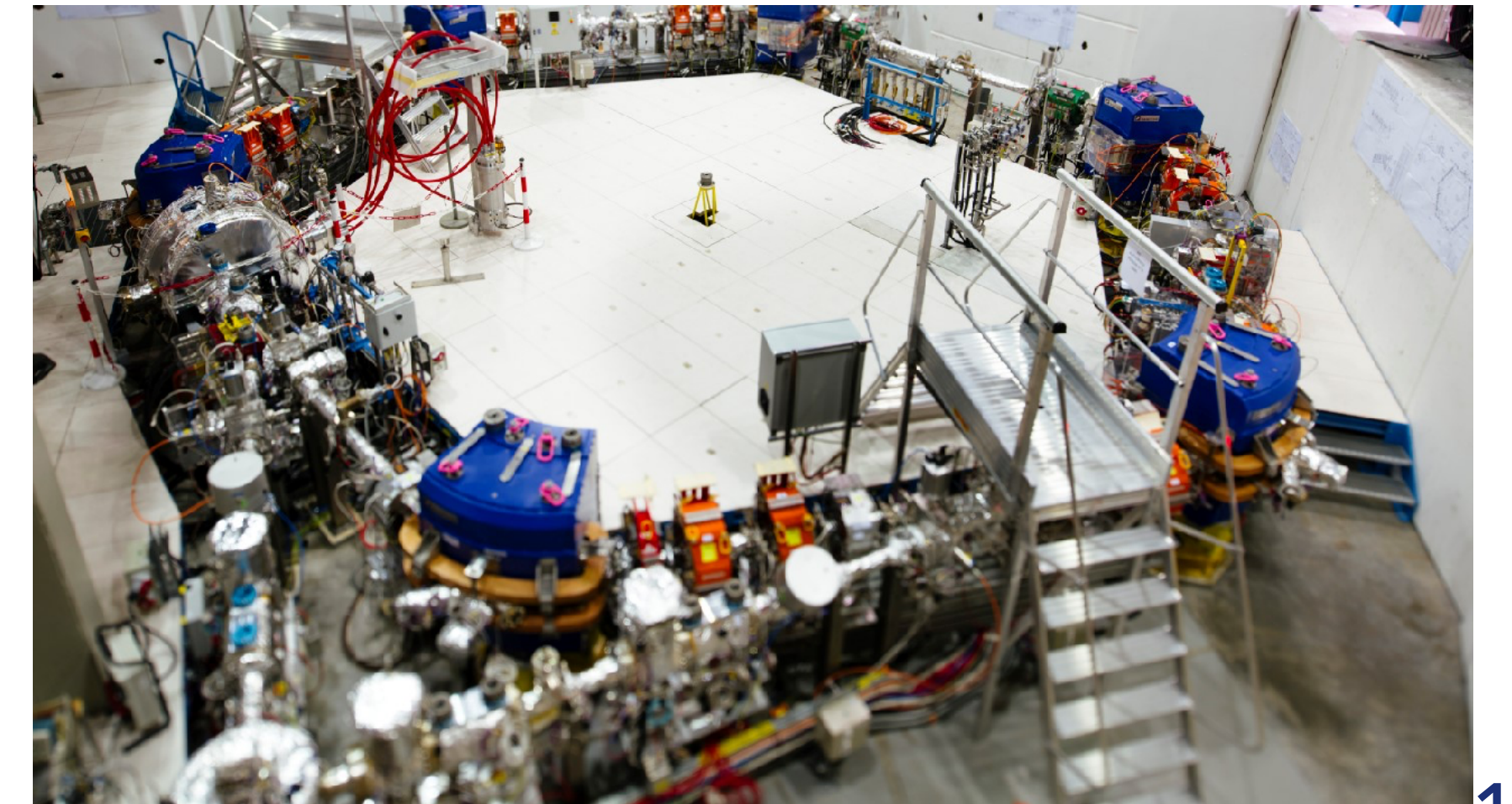
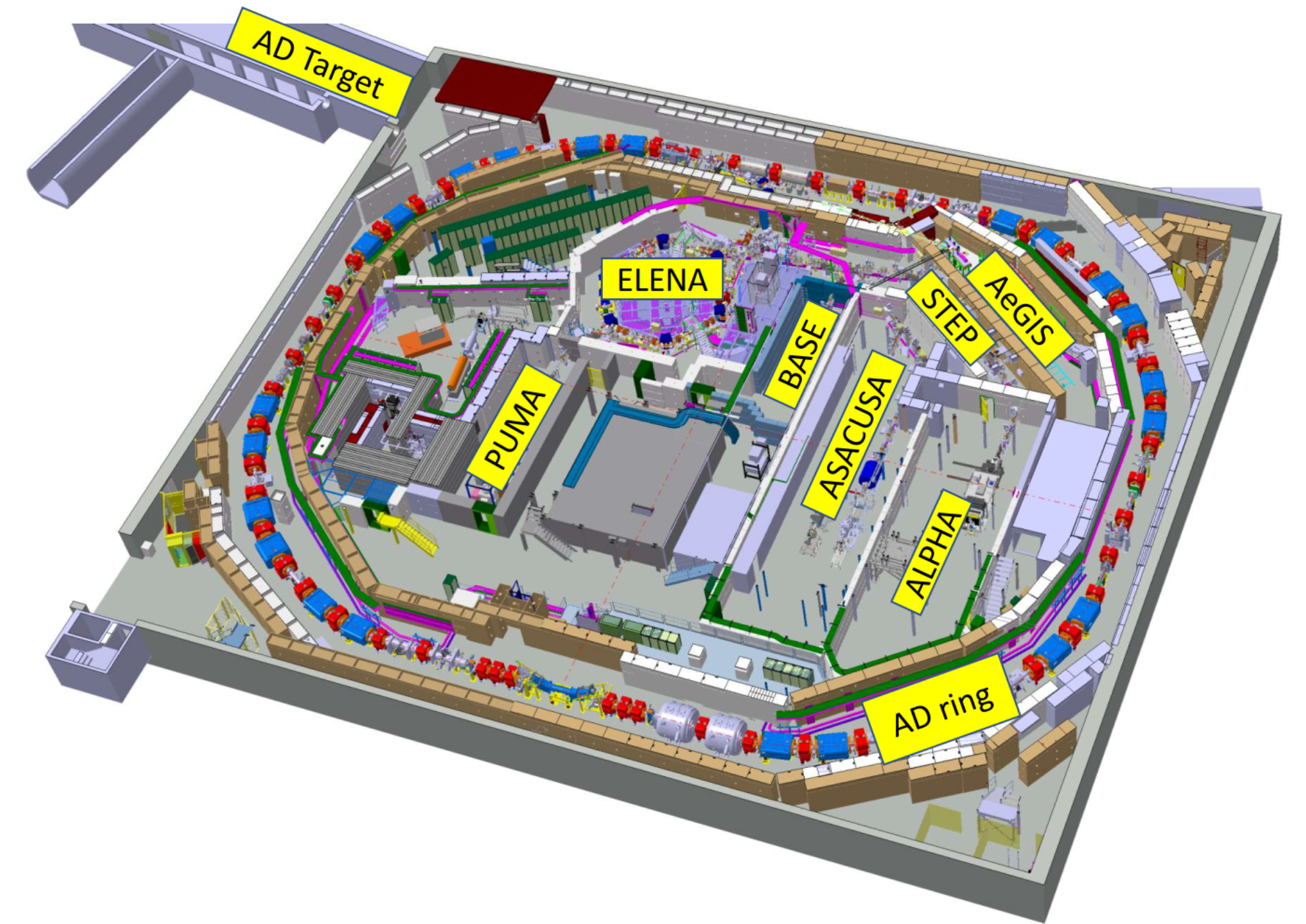
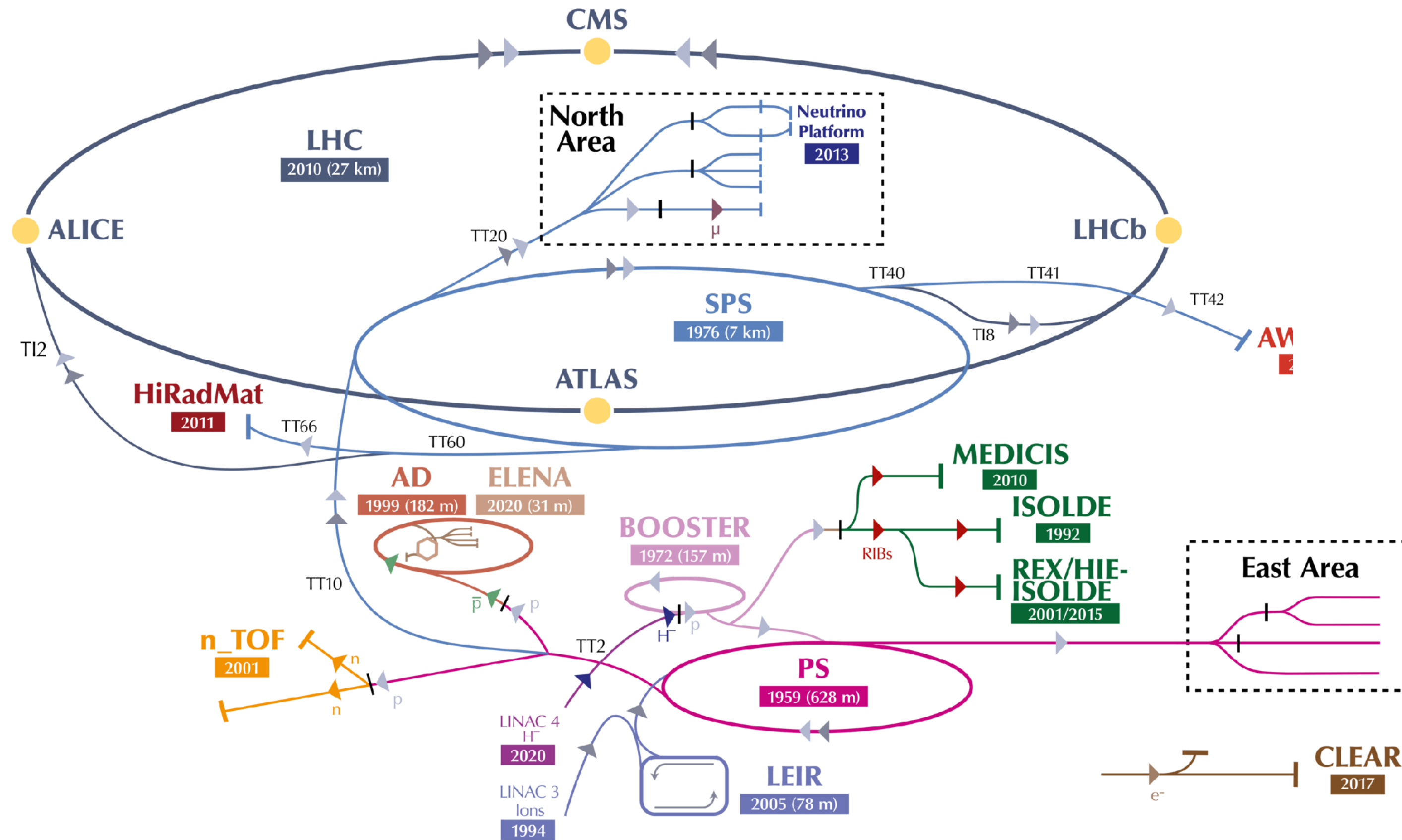
$$h(x) = \frac{1}{2} [\Psi(-ix) + \Psi(ix)] - \frac{1}{2} \ln(x^2)$$



J. Carbonell et al., PLB 397 (1997) 345

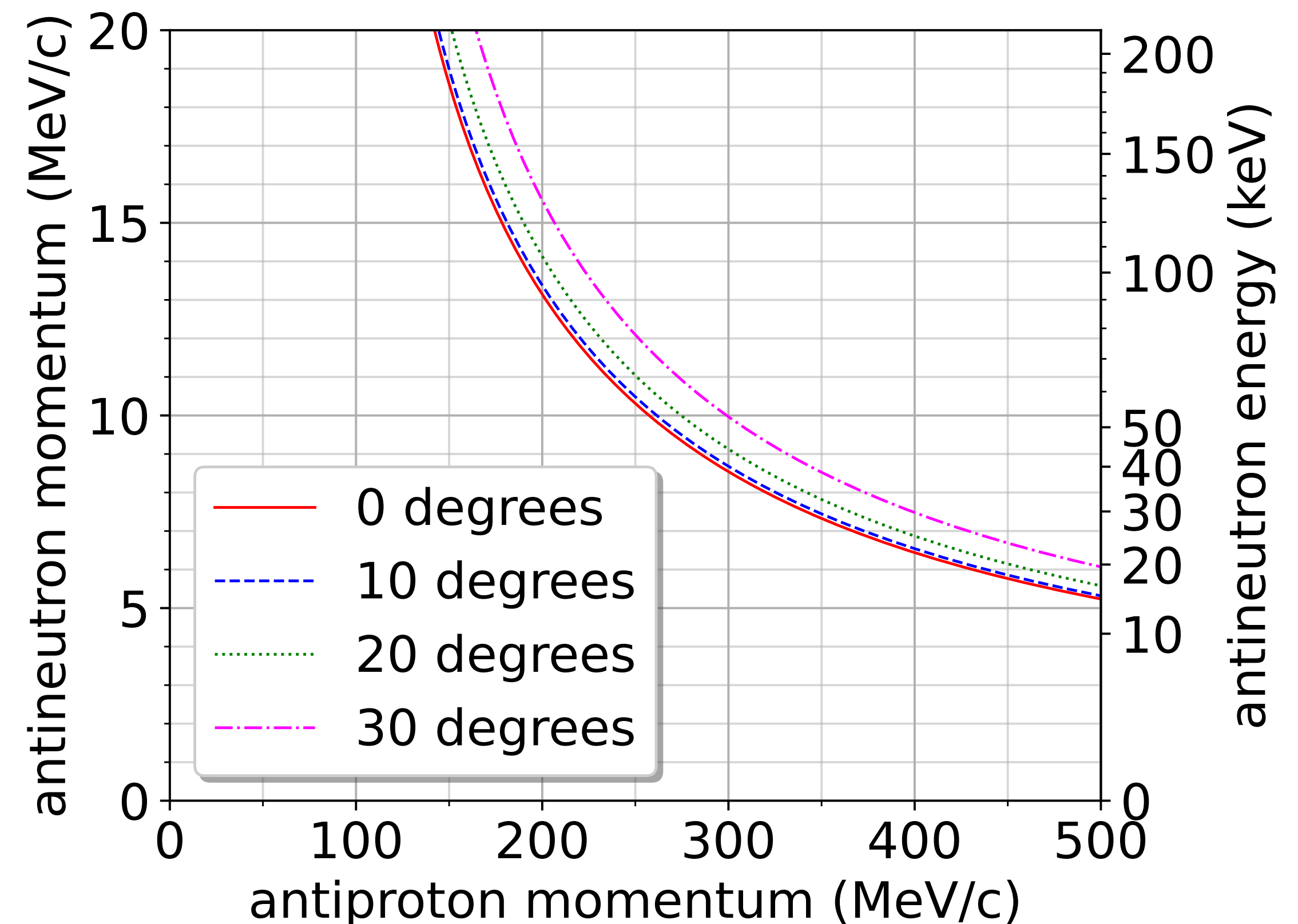
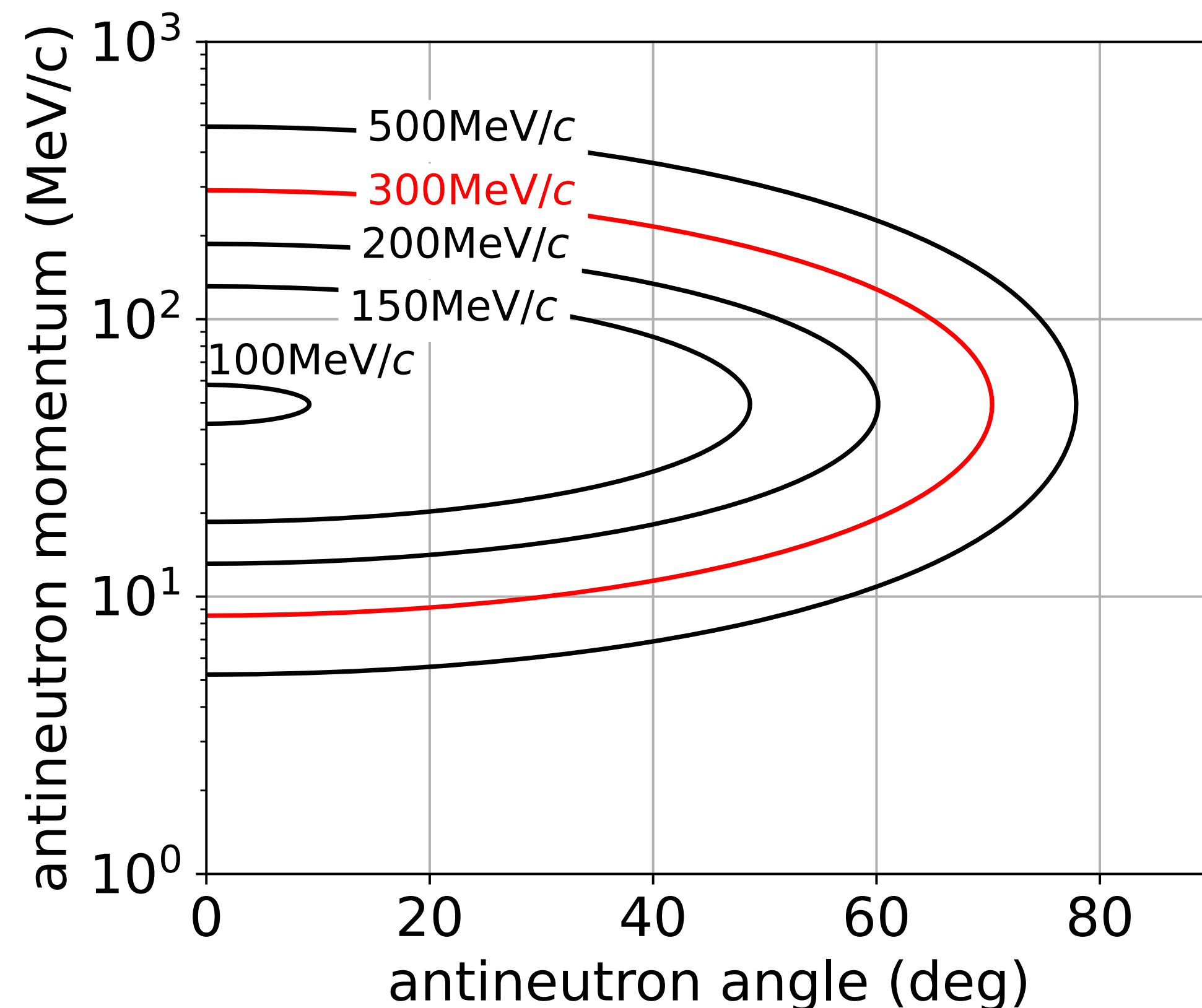
A. Zenoni et al., PLB 461 (1999) 405

CERN AD (Antiproton Decelerator)

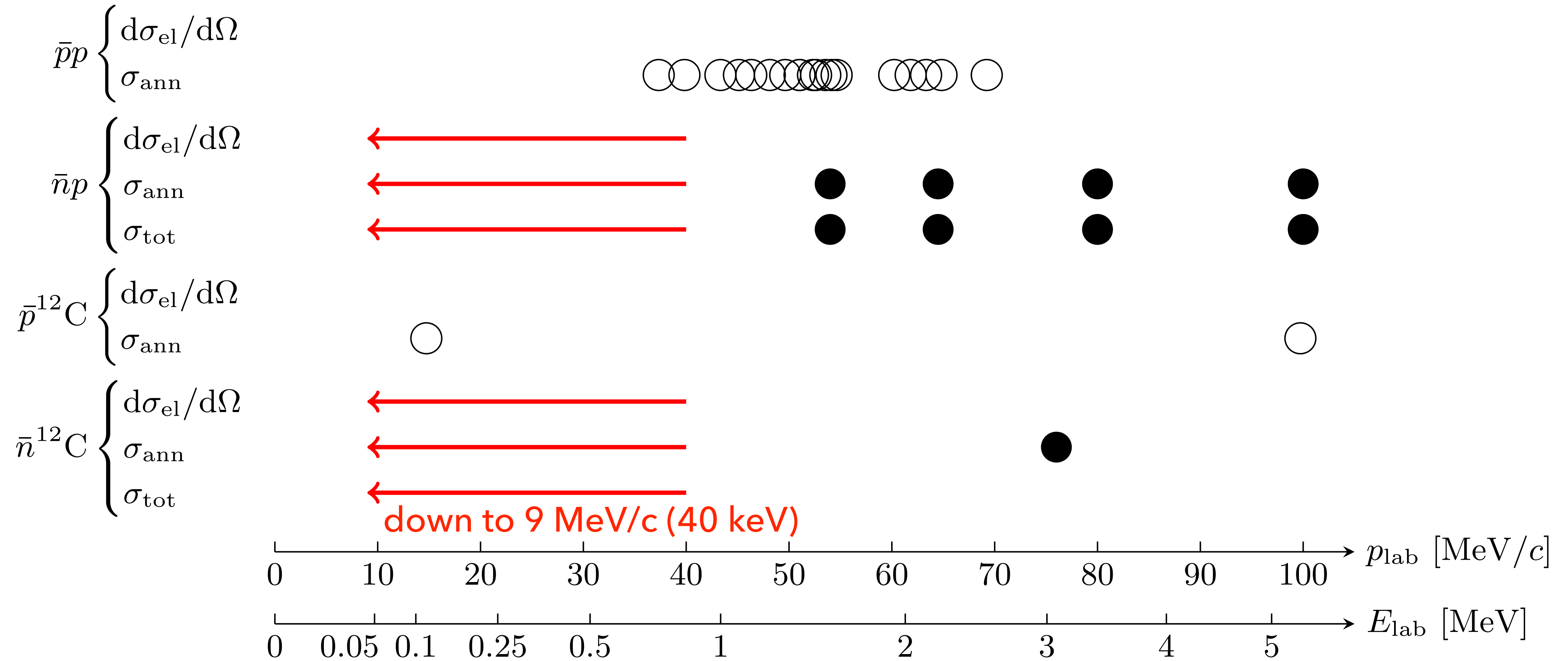


Novel concept: low-energy antineutron production

- 300 MeV/c antiprotons from CERN-AD (Antiproton Decelerator)
- $p_{\text{lab}} = 9 \text{ MeV}/c$ (40 keV) antineutrons can be backward-produced in charge-exchange reaction ($p\bar{p} \rightarrow n\bar{n}$)
- 1.0 antineutrons per cycle (~2min.) \rightarrow scattering experiments feasible



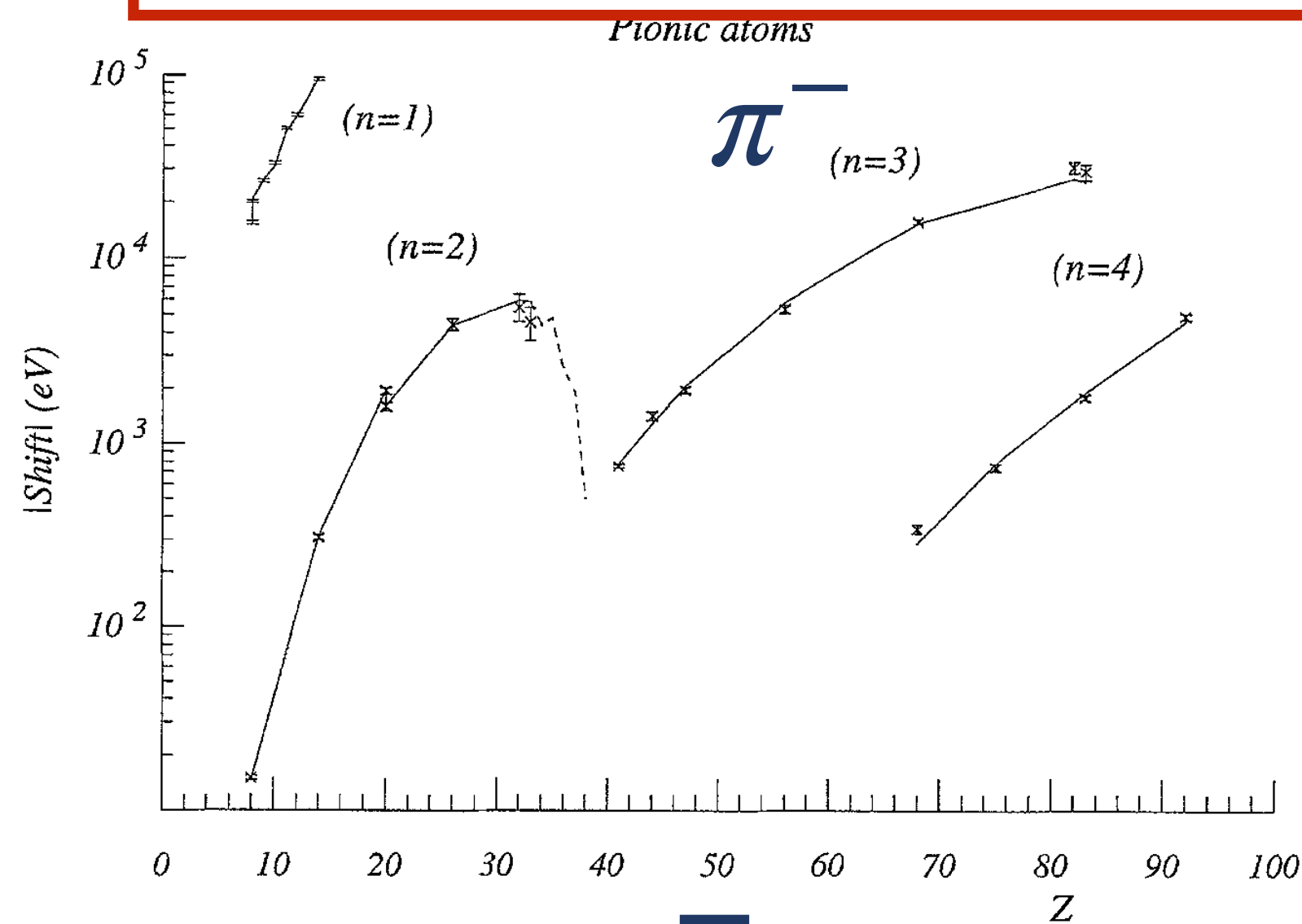
Summary of existing data and prospect



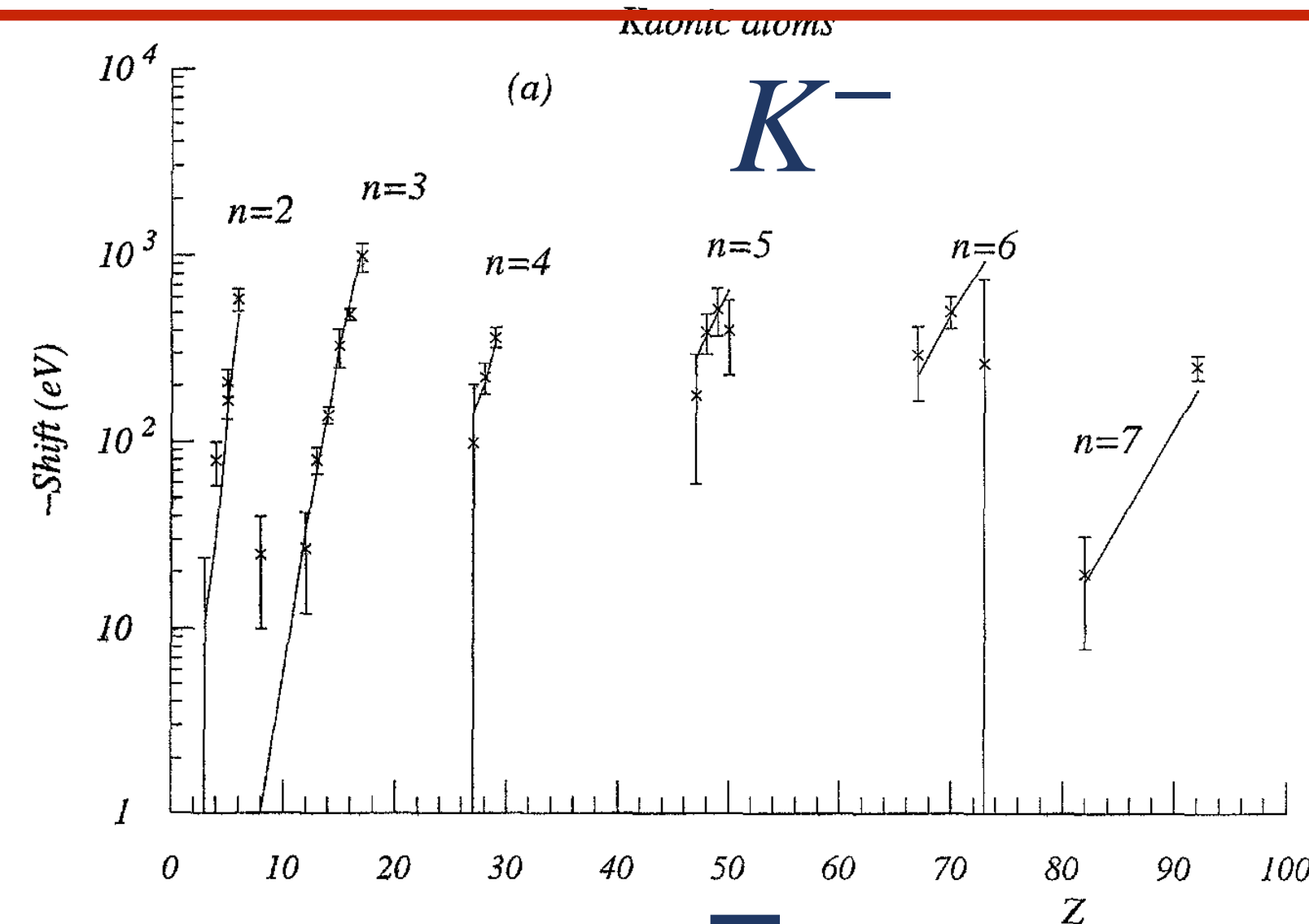
Strong interaction in exotic atoms

C.J. Batty et al., Phys. Rep. 287 (1997) 385

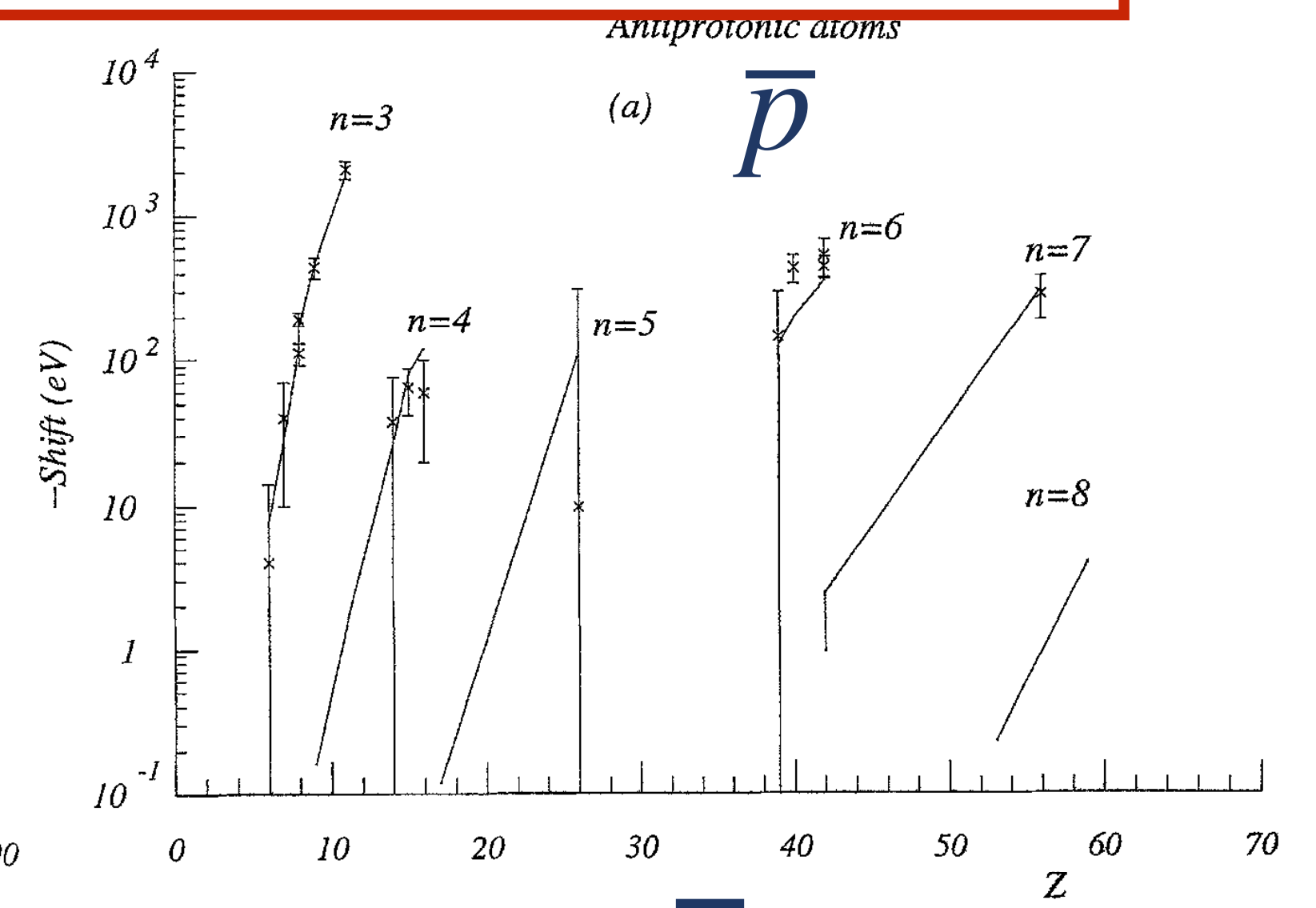
shift ($= E_{\text{measured}} - E_{\text{Coulomb}}$), width of atomic levels \rightarrow strong interaction between hadron and nucleus



- pionic hydrogen/deuterium
- deeply bound pionic atoms

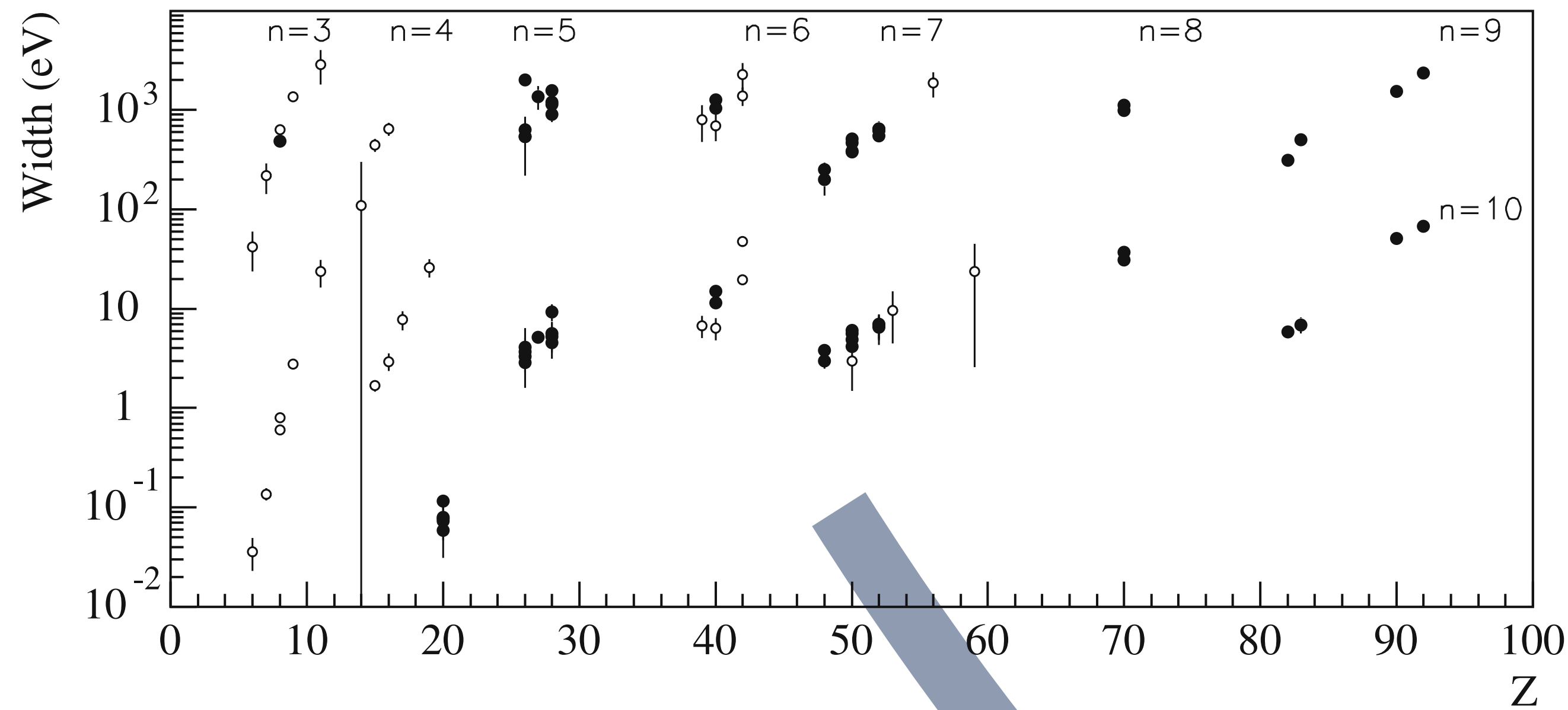


- kaonic hydrogen/deuterium
- kaonic helium-3/4

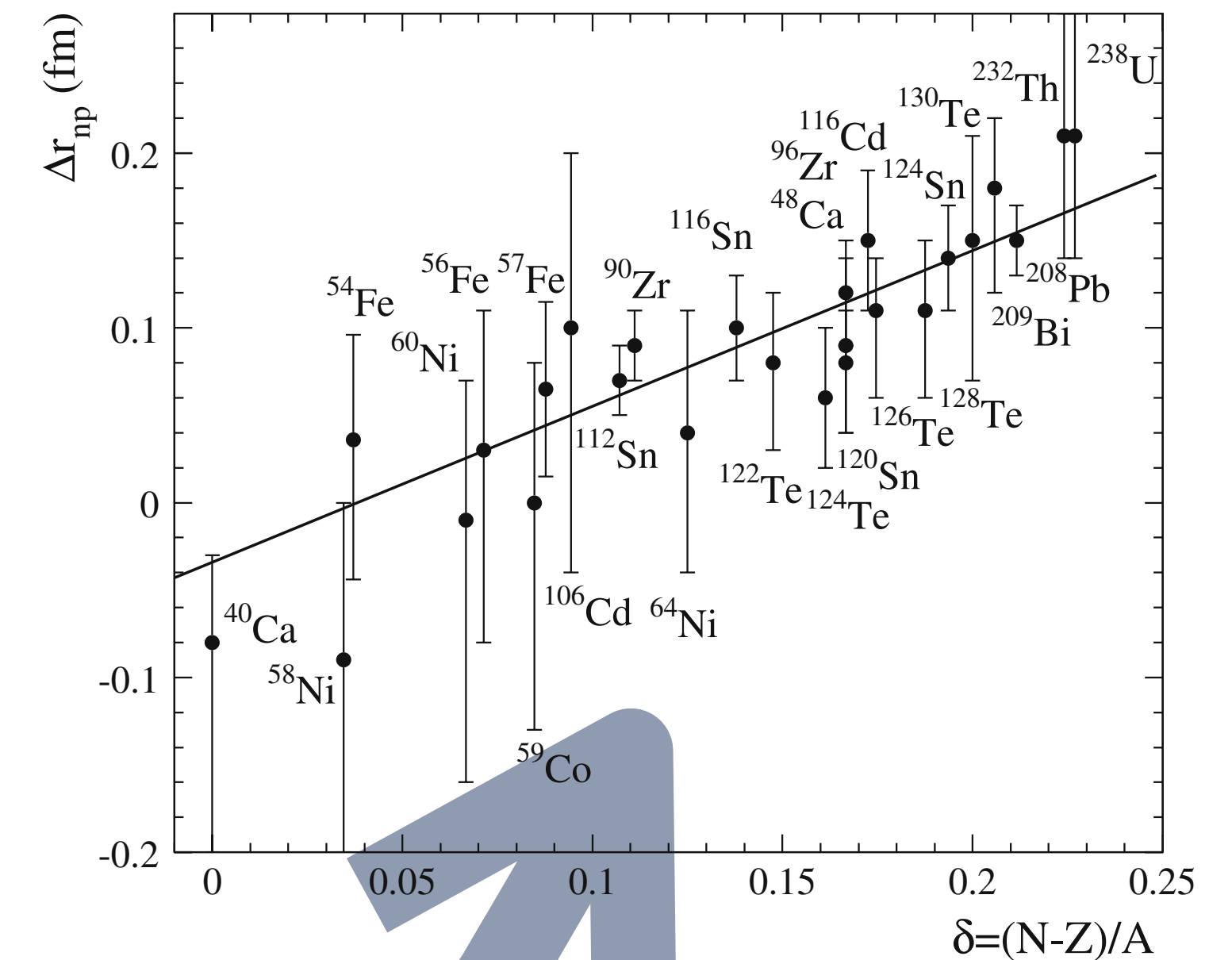


- protonium
- anti-protonic deuterium
- CERN PS209 (^{16}O , ..., ^{238}U)

A. Trzcińska et al., *Hyperfine Interact.* 194 (2009) 271



$$\Delta r_{np} = \langle r^2 \rangle_n^{1/2} - \langle r^2 \rangle_p^{1/2}$$



optical potential

$$2\mu U_{\text{opt}}(r) = -4\pi \left(1 + \frac{\mu}{m} \right) (b_0 \rho(r) + b_1 \delta\rho(r))$$

$$\rho(r) = \rho_n(r) + \rho_p(r)$$

$$\delta\rho(r) = \rho_n(r) - \rho_p(r)$$

$$b_0 = 2.5 + 3.4i \text{ (global fit)}$$

C.J. Batty et al., *Nucl. Phys. A* 592 (1995) 487

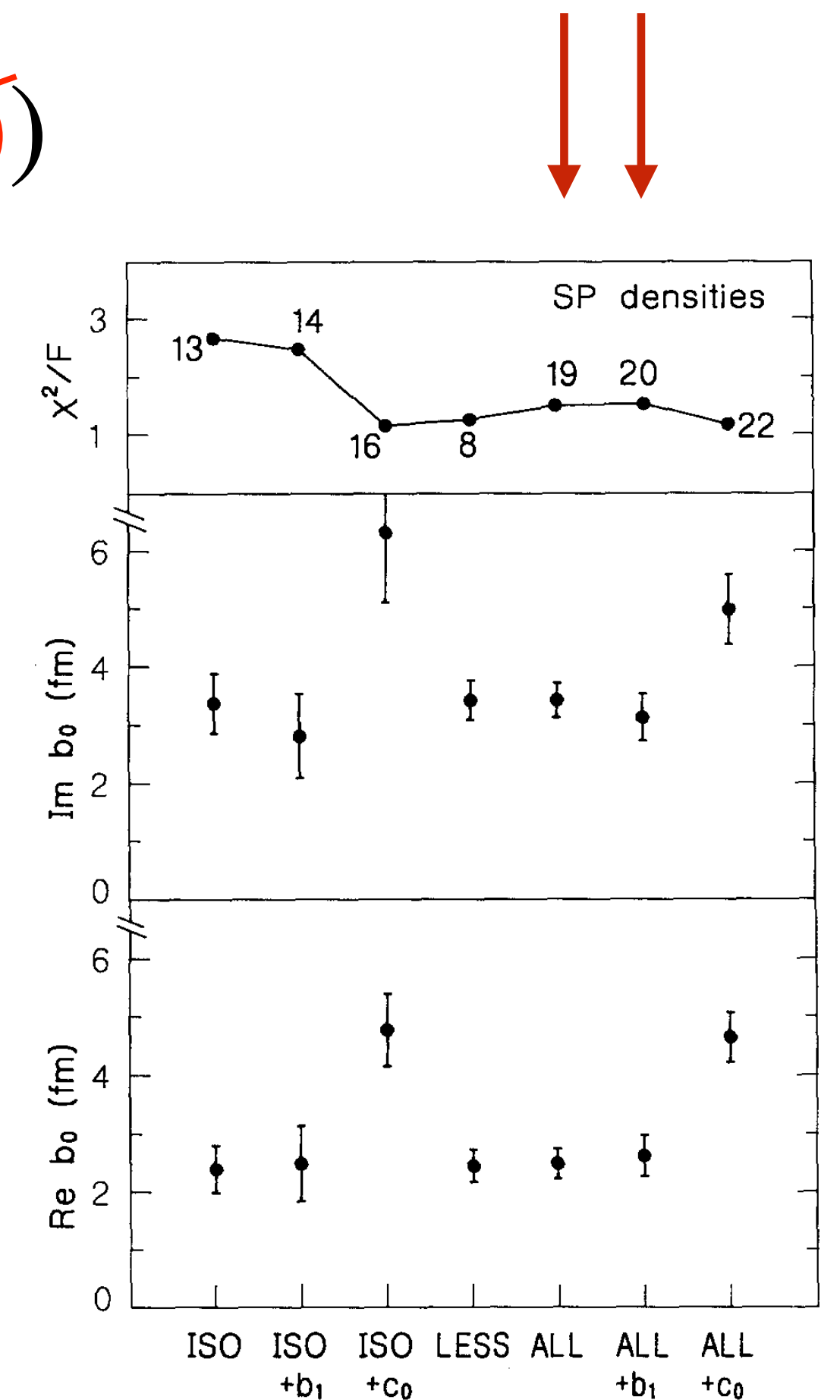
$$\rho_{n/p}(r) = \frac{\rho_0}{1 + \exp[(r - c_{n/p})/a_{n/p}]}$$

with $c_n = c_p$

Revisiting the isovector term

$$2\mu U_{\text{opt}}(r) = -4\pi \left(1 + \frac{\mu}{m} \right) (b_0\rho(r) + \cancel{b_1\delta\rho(r)})$$

- Inclusion of **the isovector (b_1) term** did not improve the χ^2/ndf in the global fit.
- Many literatures ignores the isovector term.
- Levels are sensitive only to extremely outer, low density ($< 0.1\rho_0$) regions, where neutrons dominate over protons.



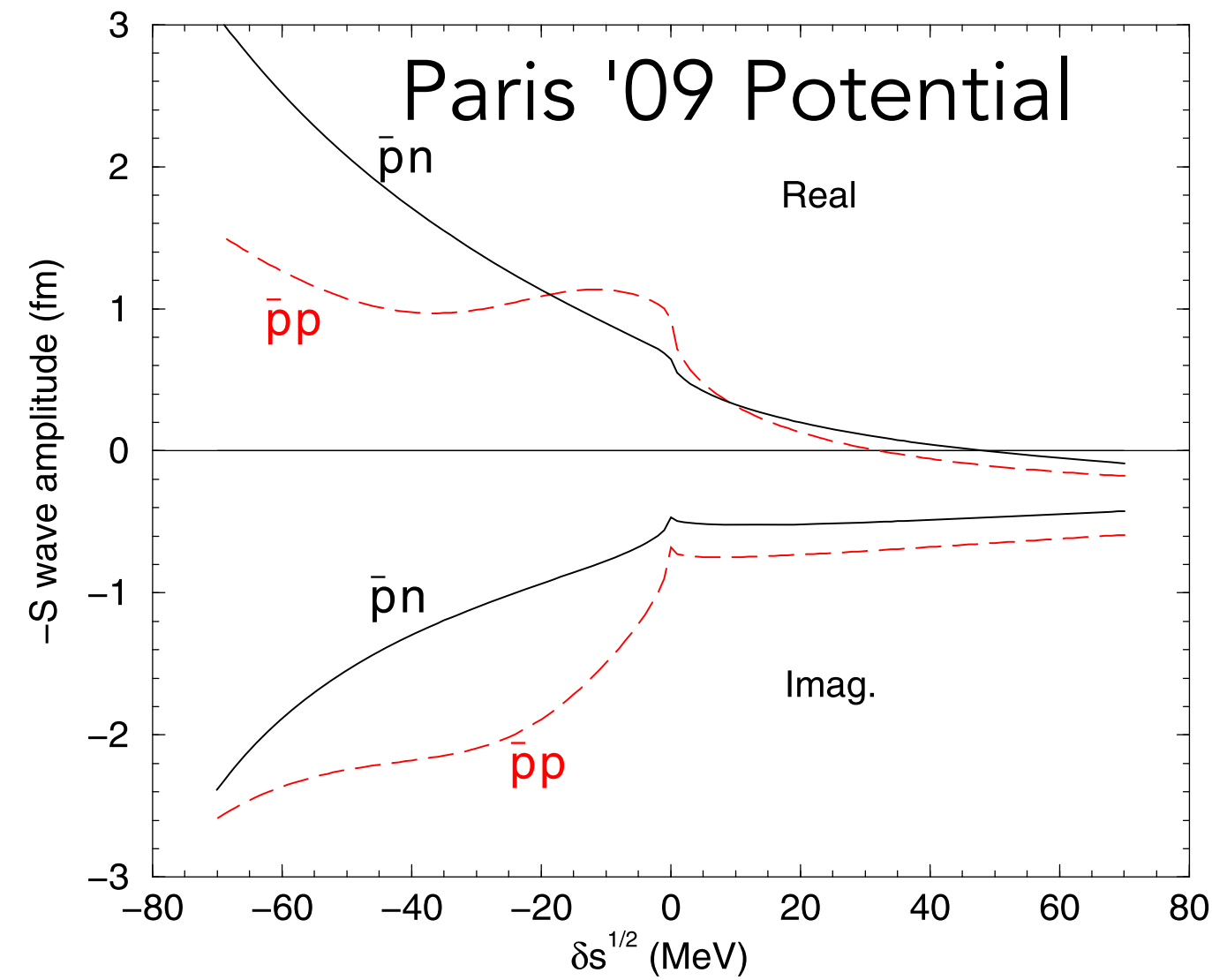
C.J. Batty et al., Nucl. Phys. A 592 (1995) 487

see also

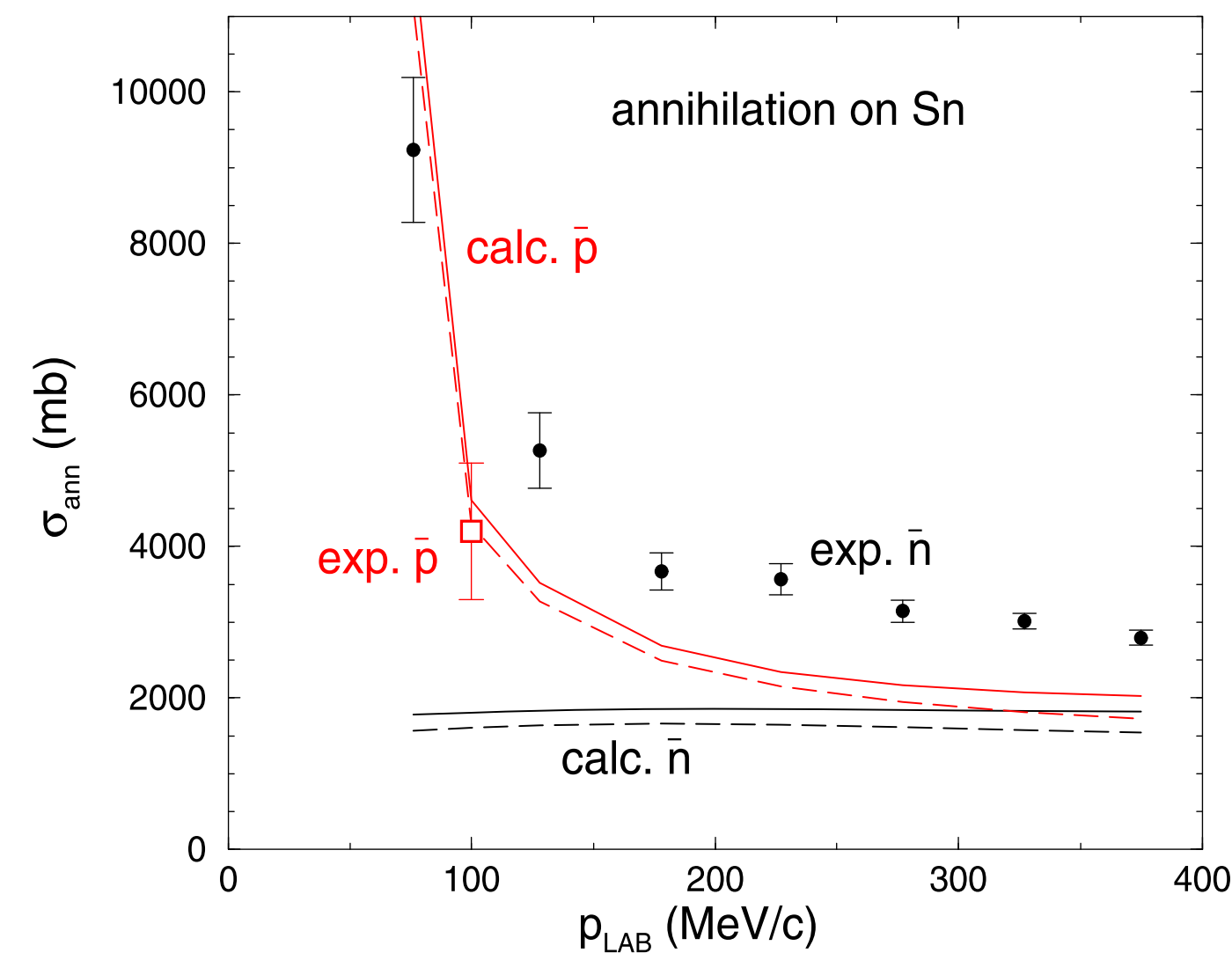
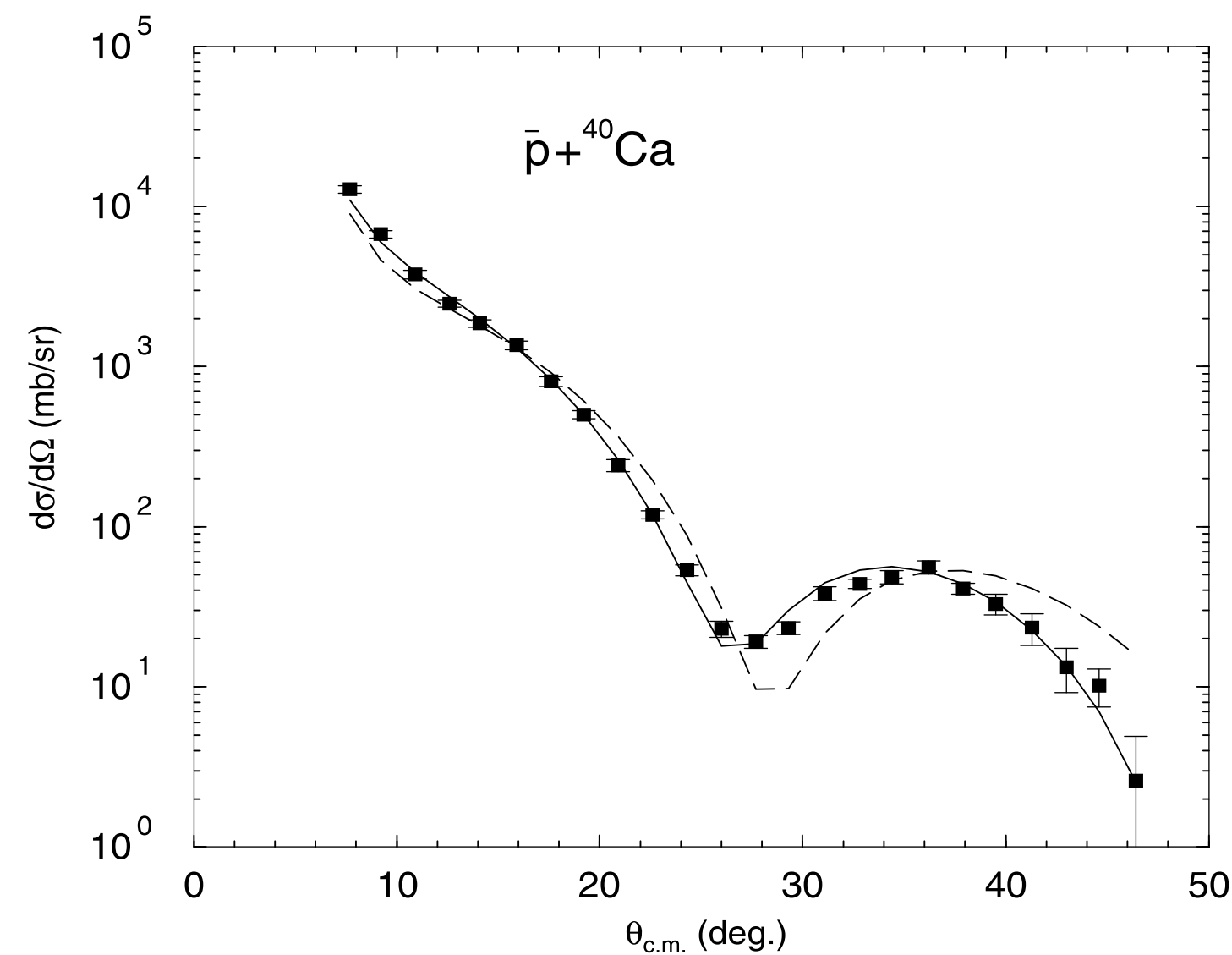
E. Friedman and A. Gal, NIM B 214 (2004) 160

E. Friedman et al., Nucl. Phys. A 761 (2005) 283

Open questions about $\bar{N}A$ interactions



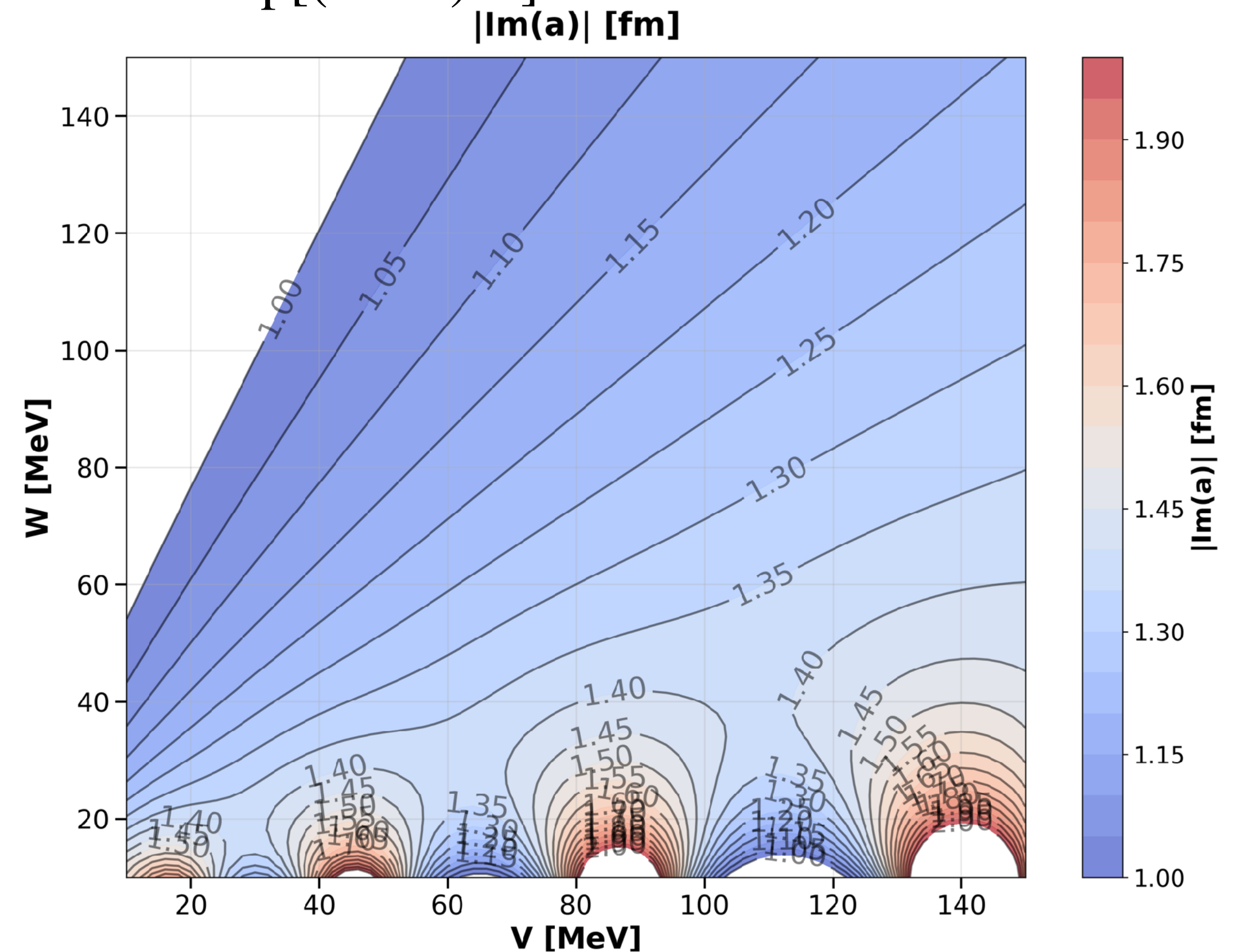
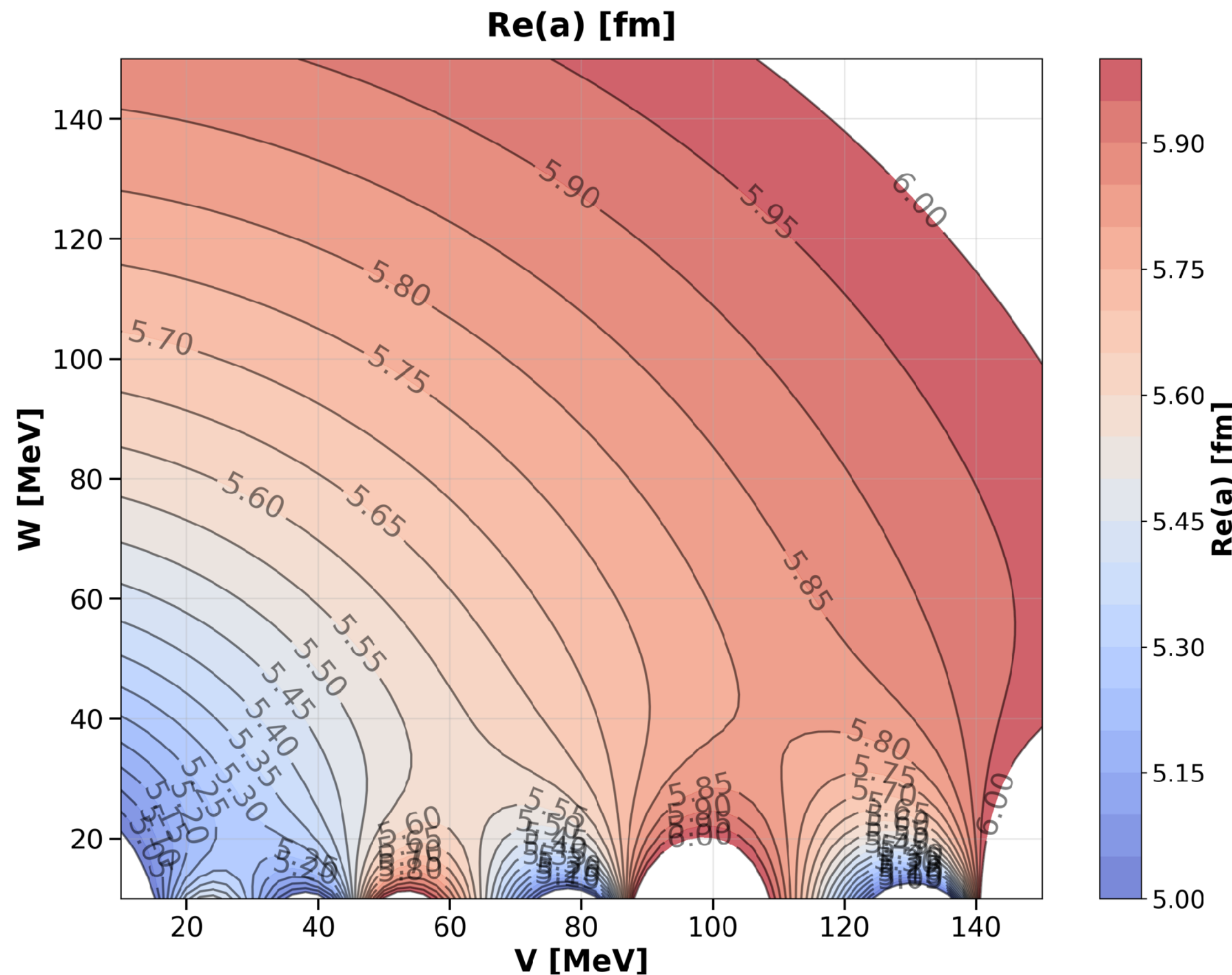
Does b_1 happen to be consistent with zero, even if $\bar{p}p$ and $\bar{p}n$ interactions are different?



$\bar{n}A$ annihilation cannot be described by the optical potential determined by a global fit for antiprotonic atoms.

Correlation between $a_{\bar{n}A}$ and optical potential

Woods-Saxon type optical potential: $V(r) = -\frac{V + iW}{1 + \exp[(r - R)/a]}$ (R=5fm, a=0.5fm)



cf. $V(r) = -\frac{2\pi}{\mu} \left(1 + \frac{\mu}{m_N} \right) b_0 \rho(r)$

→ $V \sim 103 \text{ MeV}$ and $W = 158 \text{ MeV}$ for $b_0 = 1.3 + 1.8i \text{ fm}$ (Batty et al., Nucl. Phys. A 761, 283 (2005))

for a square-well potential with $W \rightarrow -\infty$,
 $\text{Re } a \rightarrow R$ (radius) and $\text{Im } a \rightarrow 0$

Neutron-antineutron oscillation

- violates both B and B-L (B: baryon number, L: lepton number)
- test of Grand Unified Theory

- Lower limit on oscillation time

- ▷ ILL (1994) free neutron

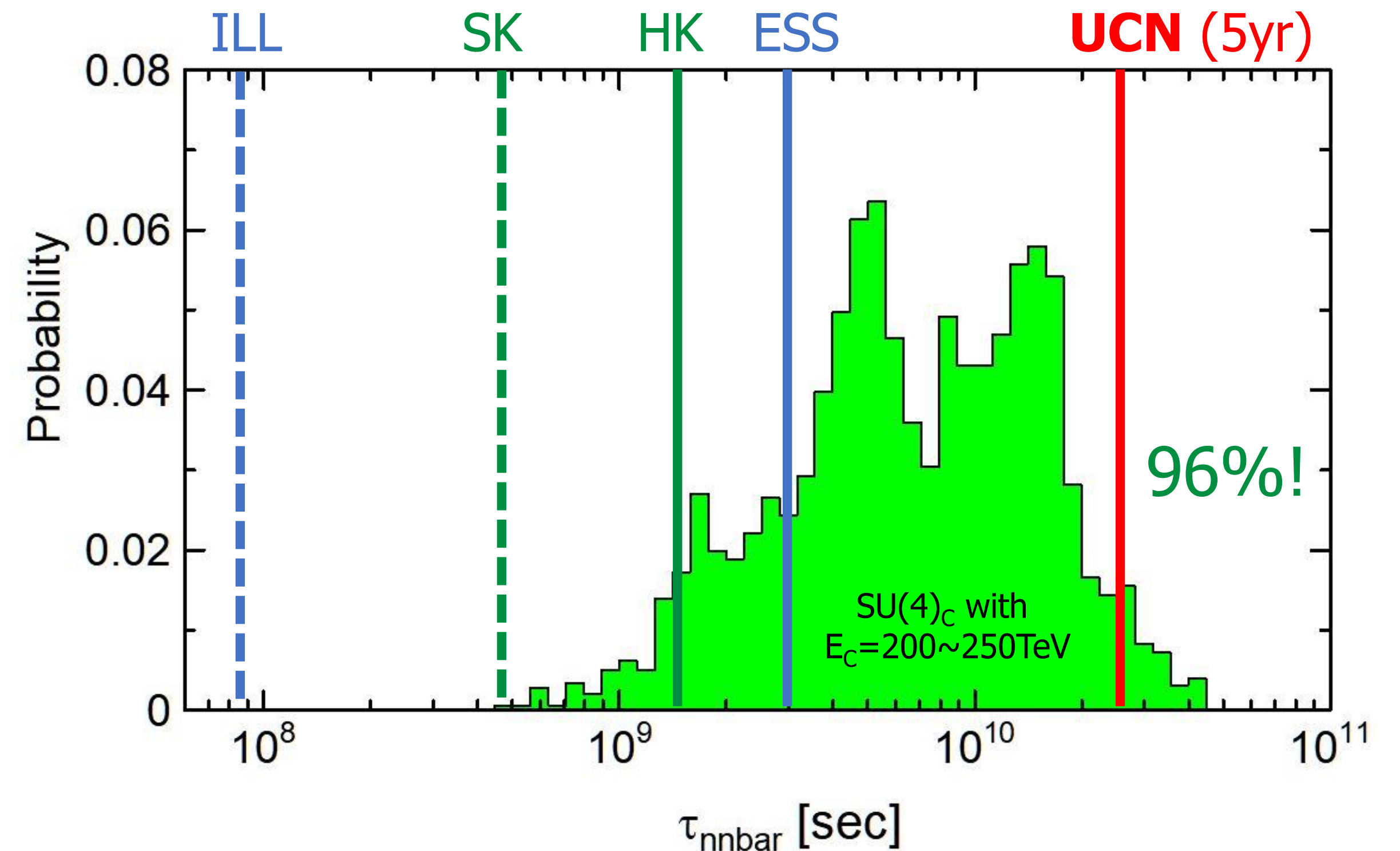
$$\tau_{n\bar{n}} > 8.6 \times 10^7 \text{ s}$$

- ▷ Super-Kamiokande (2021) bound n

$$\tau_{n\bar{n}} > 4.7 \times 10^8 \text{ s}$$

M. Baldo-Ceolin et al., Z. Phys. C 63, 409 (1994).

K. Abe et al., Phys. Rev. D 103, 012008 (2021).



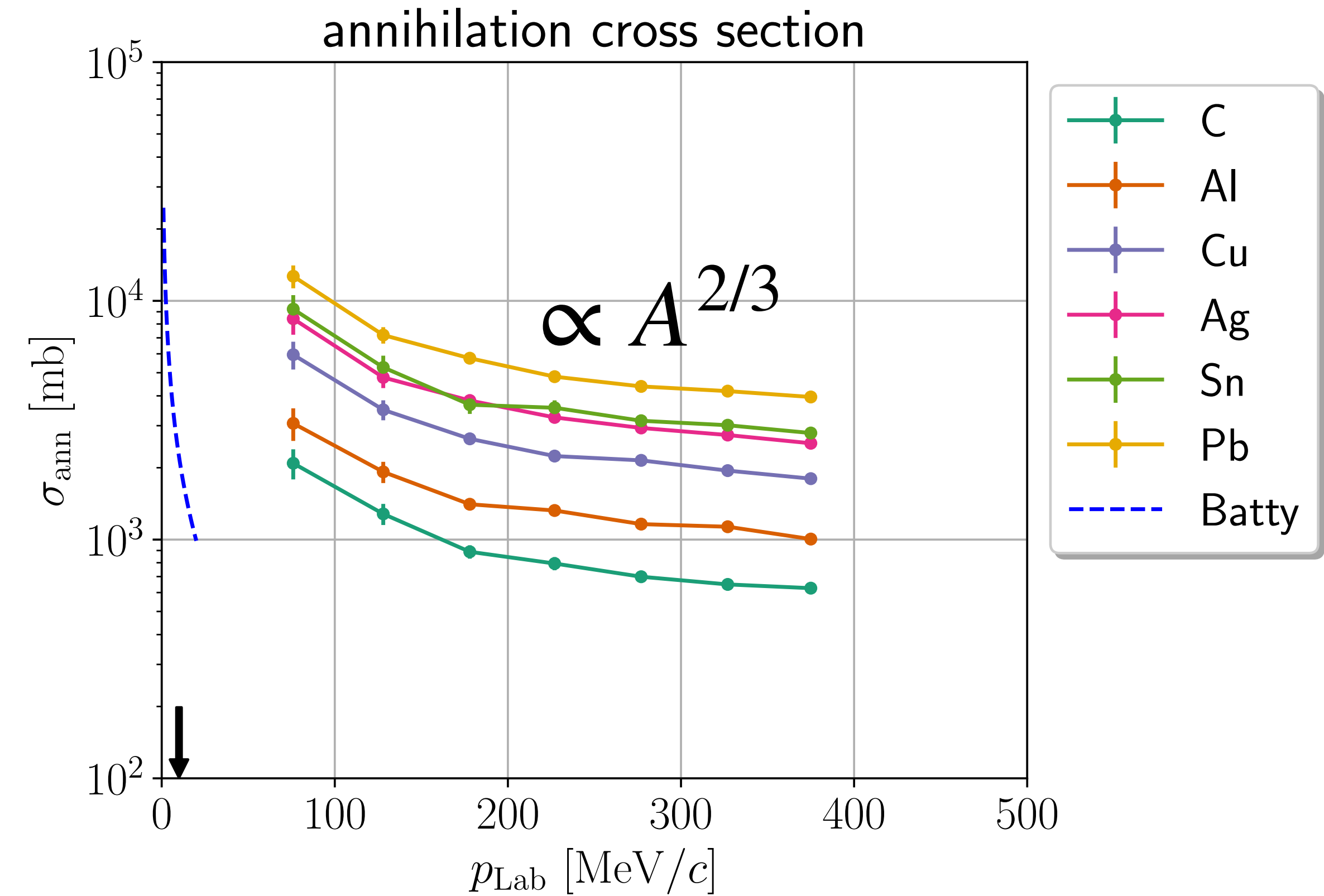
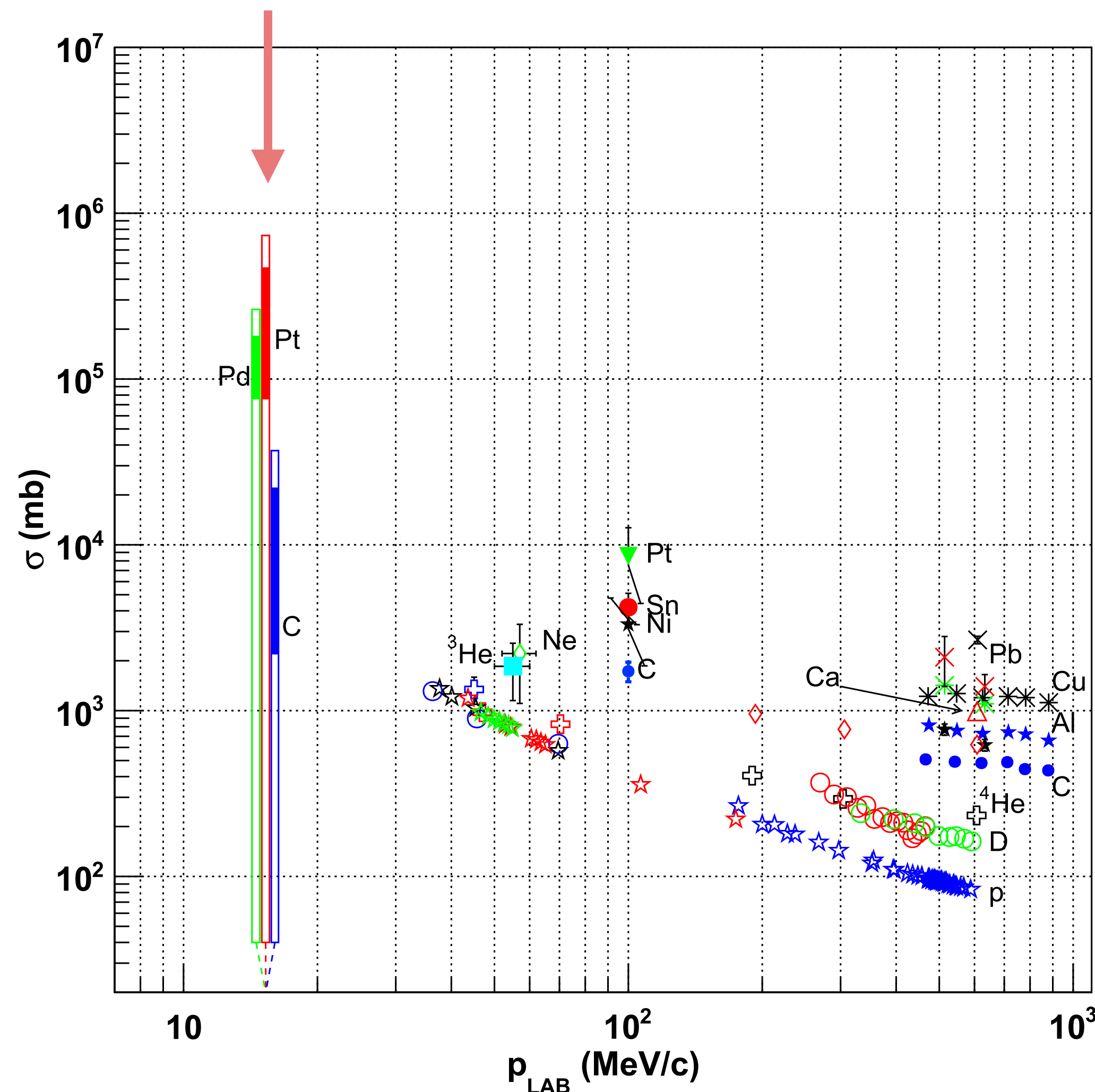
D.G. Phillips II et al., Phys. Rep. 612 (2015) 1

K.S. Babu et al., Phys. Rev. D 87 (2013) 115019

T. Shima, Symmetry 17 (2025) 1524

$\bar{p}A$ annihilation cross sections

(Coulomb-corrected) scattering length? [$\ell = R \cdot p < \hbar/2$]

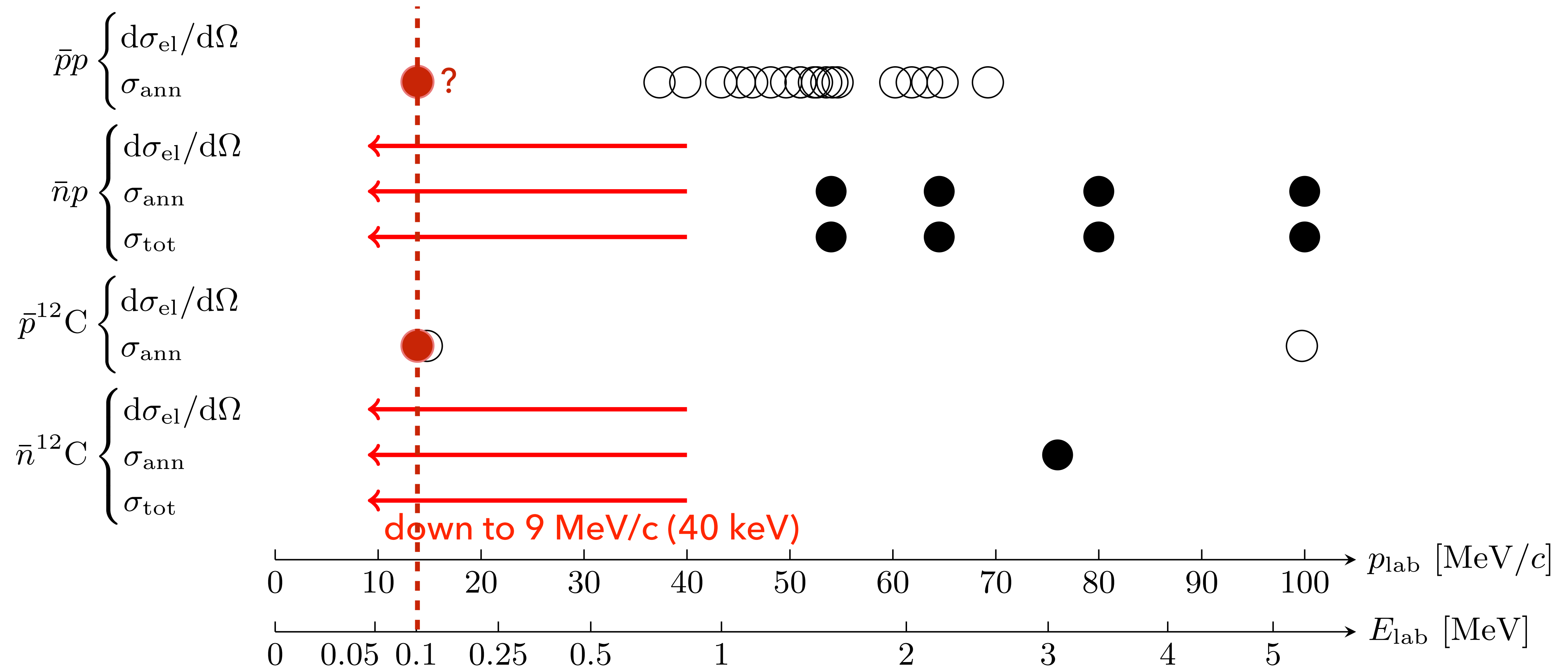


M. Astrua et al., NPA 697 (2002) 209

Aghai-Khozani et al. (ASACUSA), NPA 1009 (2021) 122170

Summary of existing data and prospect

100 keV antiprotons from ELENA



まとめ

- 様々な $NN̄$ ポテンシャルが提案されているが、それぞれ大きく異なる。
- 一部例外を除き、低エネルギー散乱断面積は採用されず。
- s波散乱断面積を用いてs波散乱長をモデル非依存に決定したい。

- 反陽子原子を再現する反陽子-原子核光学ポテンシャルは、反核子-原子核の散乱断面積をあまりよく再現しない
- アイソスピン依存性を無視した $t\rho$ 近似が原因？エネルギー依存性？
- 同じくs波散乱断面積からs波散乱長をモデル非依存に決定したい。
- s波散乱長 → 中性子-反中性子振動探索においても重要なパラメータ